Journal of South American Earth Sciences 111 (2021) 103440

Contents lists available at ScienceDirect

Journal of South American Earth Sciences

journal homepage: www.elsevier.com/locate/jsames

Evolution of a fluvial-dominated delta during the Oligocene of the Colombian Caribbean: Sedimentological and ichnological signatures in well-cores

Sergio A. Celis[a,b,*], Francisco J. Rodríguez-Tovar[b], Carlos A. Giraldo-Villegas[a,b], Andrés Pardo-Trujillo[a,c]

[a] Instituto de Investigaciones en Estratigrafía-IIES, Universidad de Caldas, Calle 65 N° 26 - 10, Manizales, 275, Colombia
[b] Departamento de Estratigrafía y Paleontología, Universidad de Granada, Avda. Severo Ochoa S/n, 18002, Granada, Spain
[c] Departamento de Ciencias Geológicas, Universidad de Caldas, Calle 65 N° 26 - 10, Manizales, 275, Colombia

A R T I C L E I N F O

Keywords:
Trace fossils
Palaeoecological and depositional conditions
Deltaic system
Well-core
Hydrocarbon exploration
Oligocene
Colombia

A B S T R A C T

Basin analysis from Colombian Caribbean is particularly important given the interest in finding hydrocarbon reservoirs, but their complex geological evolution, and the frequent lateral and vertical variation of facies difficult a conclusive characterization, highlights the need for detailed sedimentological and ichnological studies. The study succession corresponds to an interval of a well core drilled in the south of the Sinú-San Jacinto Basin (Colombian Caribbean), with 1069 ft (~326 m) thick of an Oligocene siliciclastic succession, interpreted in general terms, as deposited in a deltaic system. The integrated sedimentological/ichnological analysis allows the differentiation of dominant facies, with predominant lithologies such as conglomerates, sandstones, mudrocks, bioclastic sediments, as well as coal beds. The ichnological assemblage is low in abundance and moderately diverse, composed by *Conichnus*, *Cylindrichnus*, *Dactyloidites*, *Macaronichnus*, *Ophiomorpha*, *Phycosiphon*, *Skolithos*, *Taenidium*, *Teichichnus*, and *Thalassinoides*, as well as rhizoliths.

The complexity of the sedimentary system is reflected in its evolution throughout the Oligocene. A type succession with coarsening-upward trend was identified and it is repeated through the succession studied. It presents a general trend from bioclastic sediments (bioclastic conglomerates, sandstones and mudrocks) that pass into horizontal lamination and massive mudrocks occasionally bioturbated by *Phycosiphon*, and interbedded by mudrocks and sandstones with lenticular bedding, and the occurrence of *Teichichnus*. Above, bioturbated muddy sandstones with *Ophiomorpha*, *Taenidium*, *Thalassinoides*, and rarely *Teichichnus*, muddy sandstones with planar cross-lamination, and horizontal lamination sandstones with *Dactyloidites*, *Ophiomorpha*, *Skolithos*, and *Thalassinoides* are registered. Transition to carbonaceous mudrocks with *Teichichnus*, coal medium beds, and fine-to coarse-grained sandstones sometimes with *Macaronichnus* and/or *Ophiomorpha* is observed. Towards the top, are observed mudrocks with rhizoliths. This succession is interrupted by massive and horizontal lamination sandstones with low bioturbation index generated by the ichnological assemblage and/or by the exclusive occurrence of *Ophiomorpha* and/or *Taenidium*. Massive sandstones with erosive bases, asymmetrical ripples, and high content of organic debris are occasionally recorded. This succession reflects a progradational trend similar to those of fluvial-dominated deltaic sequences.

Detailed analysis revealed that even the fluvial processes were dominant in the deltaic system; however, local tidal and wave influence is recorded. Moreover, integration of sedimentological and ichnological information allows characterizing the evolution of the different sub-environments of the deltaic system, as prodelta bay, distal delta front, proximal delta front, distributary channels, mouth bars, and lower delta plain, and this is essential for areas of economic interest.

* Corresponding author. Instituto de Investigaciones en Estratigrafía-IIES, Universidad de Caldas, Calle 65 N° 26 - 10, Manizales, 275, Colombia.
E-mail address: sergio.celis@ucaldas.edu.co (S.A. Celis).

https://doi.org/10.1016/j.jsames.2021.103440
Received 5 February 2021; Received in revised form 10 June 2021; Accepted 17 June 2021
Available online 26 June 2021
0895-9811/

1. Introduction

Deltaic environments are complex settings determined by the interactions of fluvial and marine hydrodynamic processes, as well as by the geometry of the receiving basin, and type and amount of sediments delivered from the river (Tonkin, 2012). In this sense, deltas generate variable coastal morphologies depending on their genesis and fluvial, tidal and/or wave interactions (Dalrymple et al., 1992).

Deltas present diagnostic facies trends as the fluvial system incorporated into the sedimentary basin supplies a greater sediment load than can be redistributed outside the mouth bar by the dominant wave and/or tidal processes, and significantly influence associated coastal environments such as coastal plains and tidal flats (Galloway, 1975; Boyd et al., 1992; Orton and Reading, 1993; Bhattacharya and Giosan, 2003; Bhattacharya, 2006). These trends are observed in outcrops and cores, being generally recognized as coarsening upward successions (Tonkin, 2012). These are progradational, and sometimes retrogradational, siliciclastic sequences associated with the dynamic of the relative sea level (regressive and transgressive phases), according to the supply of sediment, redistribution capacity, the morphology of the basin, and the coastline (Bhattacharya and Walker, 1992; Dalrymple et al., 1992; Dalrymple and Choi, 2007; Ainsworth et al., 2008, 2011, 2011; Tonkin, 2012).

The study of deltaic deposits has been based, fundamentally, on the analysis of sedimentary features (e.g., sedimentary structures, textures), together with paleontological and geochemical information (MacEachern et al., 2005). In most researches, the presence of biogenic sedimentary structures is indicated, which, according to the growth of ichnology in recent years, determined the integration of ichnological studies as an essential tool for the analysis of deltaic systems (Pemberton and Wightman, 1992; MacEachern et al., 2005; Gani et al., 2007; MacEachern and Bann, 2008, 2020; Dashtgard et al., 2011; Buatois et al., 2012; Tonkin, 2012; Shchepetkina et al., 2019; Bayet-Goll and Neto de Carvalho, 2020; Canale et al., 2020; Moyano Paz et al., 2020). Coastal systems with deltaic influence are characterized by receiving fluvial discharges that, depending on the capacity of marine processes (waves or tides) to redistribute sediment and the fresh water provided by rivers, generate significant fluctuations in the physical-chemical conditions, determining a stressful environment (Collins et al., 2019). Thus, the trace makers, as responding to these environmental changes (ecological and depositional), provides ichnological evidences (i.e., morphology and size of the structures, degree of bioturbation, distribution, ichnodiversity, ichnodisparity, tiering) which contribute to the detail characterization of delta settings (Ekdale et al., 1984; Bromley, 1990; Buatois et al., 2005, 2012, 2012; MacEachern et al., 2005; Hansen and MacEachern, 2007; Bann et al., 2008; Collins et al., 2019). On this basis, the integration of sedimentology and ichnology reveals essential for the interpretation of deltaic environments, and the associated physicochemical parameters such as salinity, hydrodynamics, sedimentation rate, oxygenation, substrate consistency, turbidity, light, or temperature, allowing evaluation of the importance of fluvial, tidal and/or wave processes during delta development (Bhattacharya and Giosan, 2003; MacEachern et al., 2005, 2007a, 2007a; Gani et al., 2007; Buatois and Mángano, 2011).

The Sinú-San Jacinto (SSJB) and Lower Magdalena Valley (LMV) basins of the Colombian Caribbean have currently a particular economic importance, based on the existence of numerous oil and gas seeps, as well as boreholes with evidence of hydrocarbon (Bernal– Olaya et al., 2015; Osorno and Rangel, 2015). Particularly, the SSJB shows evidence of the existence of an active petroleum system, being one of the basins with more petroleum seeps in Colombia, and within which have been tested Upper Cretaceous sequences as hydrocarbon source rocks (Osorno and Rangel, 2015). These characteristics make this basin an ideal area for hydrocarbon exploration.

For this purpose, the National Hydrocarbons Agency (ANH) has drilled several cores of exploratory wells in order to know and understand in detail the petroleum systems of the Colombian Caribbean, because its stratigraphic and structural complexity difficult to understand the geologic evolution of the basin (e.g., Taboada et al., 2000; Cediel et al., 2003; Pindell et al., 2005; Escalona and Mann, 2011; Cardona et al., 2012; Rosello and Cossey, 2012; Alfaro and Holz, 2014; Mora et al., 2017, 2018; Silva– Tamayo et al., 2017; Montes et al., 2019). The stratigraphic studies involving the geological evolution of the SSJB show the difficulty for the establishment of the elements of the petroleum system given the continuous variation of facies both lateral and vertically (Duque– Caro, 1991; Guzmán et al., 2004; Guzmán, 2007; Bermúdez et al., 2009; Bermúdez, 2016; Mora et al., 2017, 2018; Osorio-Granada et al., 2020; Manco– Garc é s et al., 2020).

In 2015, the National Hydrocarbons Agency (ANH) drilled the ANH-SSJ-Nueva Esperanza-1X stratigraphic well, which is located close to the Montería-Planeta Rica road (coordinates 8°31′42,68″N/75°40′31,93″W) reaching a total depth of ~2266 ft (~691 m) (Fig. 1). A well core interval drilled a sedimentary succession of Oligocene age associated with Ciénaga de Oro Formation (Fig. 1) that, according to its lithological characteristics, have been considered as a potential reservoir within the system (Flinch, 2003; Marín et al., 2010). However, its complex lateral variation of facies within the basin prevents the proposal of a definitive model. On this base, the aim of the present research is the detailed integrative ichnological and sedimentological analysis of a sedimentary succession drilled in the SSJB in order to improve the understanding vertical variations, and characterization of the dynamics of deltaic environments developed in the Colombian Caribbean during the Oligocene.

2. Geological setting

The NW corner of South America is influenced by the interaction between Nazca, Caribbean and South America plates (Montes et al., 2019; Mora-Paez et al., 2019). This complex interaction has controlled the filling of the sedimentary basins from the Upper Cretaceous to the Recent (Mora et al., 2017, 2018, 2018; Montes et al., 2019; Pardo– Trujillo et al., 2020).

Into the onshore sedimentary basins at the north of Colombia, the SSJB and LMV are considered forearc basins, geologically separated by the Romeral Fault System (Bernal– Olaya et al., 2015; Mora et al., 2018; Montes et al., 2019). The SSJB is located on an igneous oceanic basement of Cretaceous age (Geotec, 2003; Guzmán, 2007; Bermúdez et al., 2009; Silva– Arias et al., 2016; Mora et al., 2017). Its sedimentary fill includes rocks from Upper Cretaceous to Recent (Fig. 2), linked to the northeastern migration of the Caribbean Plate (Mora et al., 2017, 2018; Montes et al., 2019; Pardo– Trujillo et al., 2020). Limestones, mudrocks, cherts and sandstones, from the Cansona Formation of Campanian – Maastrichtian age overlay the basement (Duque-Caro, 1968, 1972; Guzmán, 2007; Bermúdez et al., 2009; Dueñas and Gomez, 2011; Bermúdez, 2016). Subsequently, the collision of the Caribbean Plateau against the northern South American margin produced a tectonic event, recognized by a lower Paleocene unconformity-LPU (Guzmán et al., 2004; Mora et al., 2017). Upper Paleocene – lower Eocene conglomerates, sandstones and mudrocks from the San Cayetano Formation overlay the Upper Cretaceous rocks (Duque-Caro, 1972; Guzmán, 2007; Bermúdez et al., 2009; Bermúdez, 2016; Mora et al., 2017). In the early to middle Eocene, the increase in morphotectonic activity generated another unconformity: lower middle Eocene unconformity-LMEU (Guzmán et al., 2004; Mora et al., 2017). The Chalan/Chengue/Toluviejo formations, composed of conglomerates, sandstones, limestones and mudrocks of middle – late Eocene age overlay the San Cayetano Formation, and are overlaid by the Carmen/San Jacinto formations of late Eocene – early Oligocene age (Duque-Caro, 1972; Guzmán, 2007; Bermúdez et al., 2009; Bermúdez, 2016; Mora et al., 2017, 2018). Later, sandstones and siltstones with coal beds associated with the Ciénaga de Oro Formation (Oligocene – early Miocene age) were deposited (Duque-Caro, 1972; Guzmán, 2007; Bermúdez et al., 2009; Bermúdez,

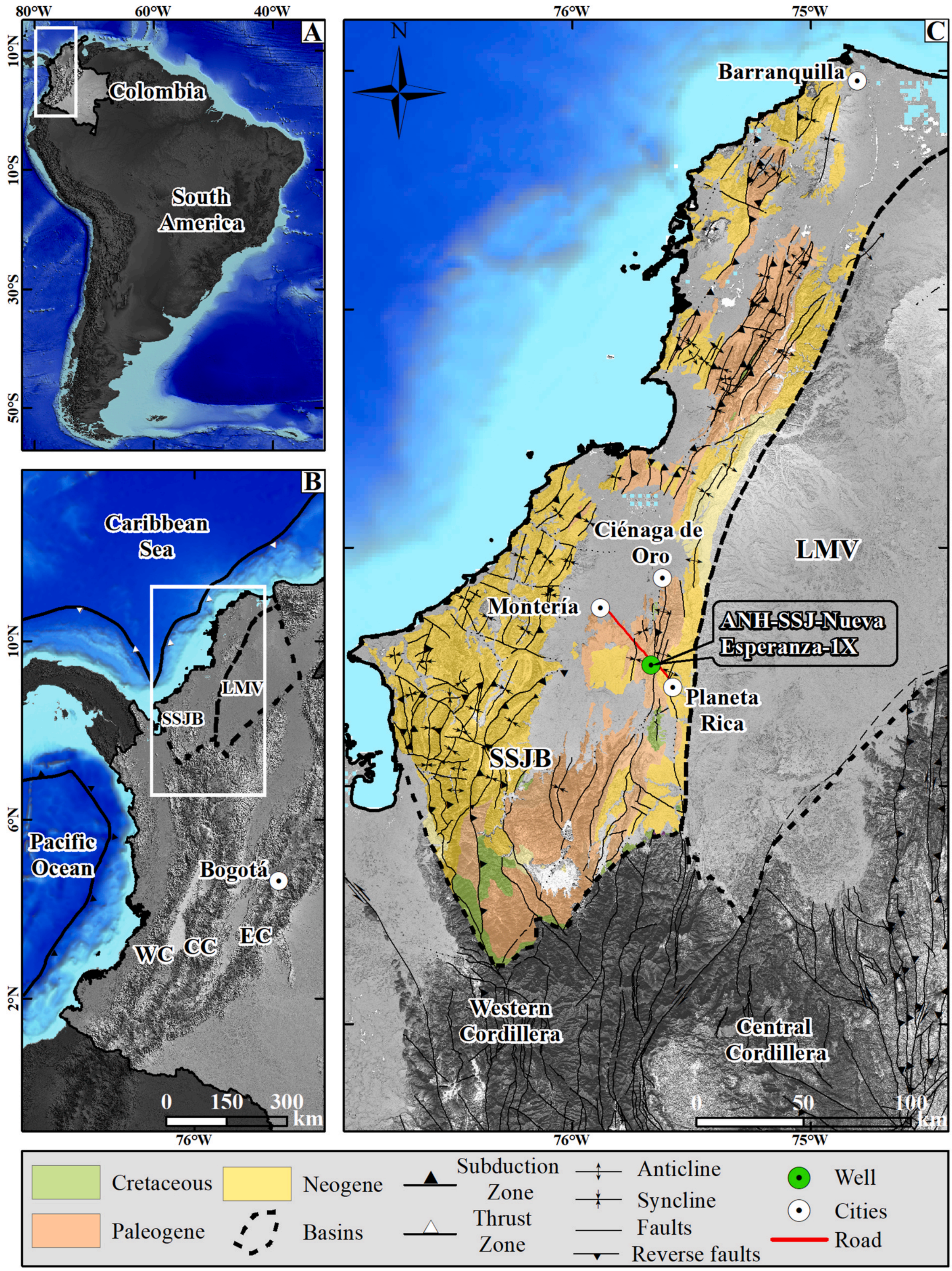

Fig. 1. Location map. **A.** Location of Colombia in South America. **B.** Location of the Sinú-San Jacinto Basin (SSJB) and Lower Magdalena Valley Basin (LMV) in the Colombian Caribbean (WC Western Cordillera; CC Central Cordillera; EC Eastern Cordillera). **C.** Sinú-San Jacinto Basin (SSJB). Montería-Planeta Rica road. Geology is only indicated in the SSJB (Source: WGS-1984 coordinate system; CIOH, SRTM, NOAA elevation and ocean models; geology of Gómez et al., 2015).

2016; Mora et al., 2017, 2018; Manco– Garc é s et al., 2020). A regional early Miocene tectonic event generated the lower Miocene unconformity-LMU (Mora et al., 2018). In the middle to late Miocene, were deposited siltstones and in minor proportion sandstones correspond to the Porquero Formation (Duque-Caro, 1972; Guzmán, 2007; Bermúdez et al., 2009; Bermúdez, 2016). Upper Miocene – Pliocene sandstones, siltstones and carbonaceous levels associated with the El Descanso, El Cerrito and Tubará Formation were registered above (Duque-Caro, 1972; Guzmán, 2007; Molinares et al., 2012). Finally, Pliocene and Quaternary sandstones, siltstones, conglomerates and limestones from the Sincelejo, Morroa and La Popa Formation were deposited (Duque-Caro, 1972; Guzmán, 2007; Molinares et al., 2012).

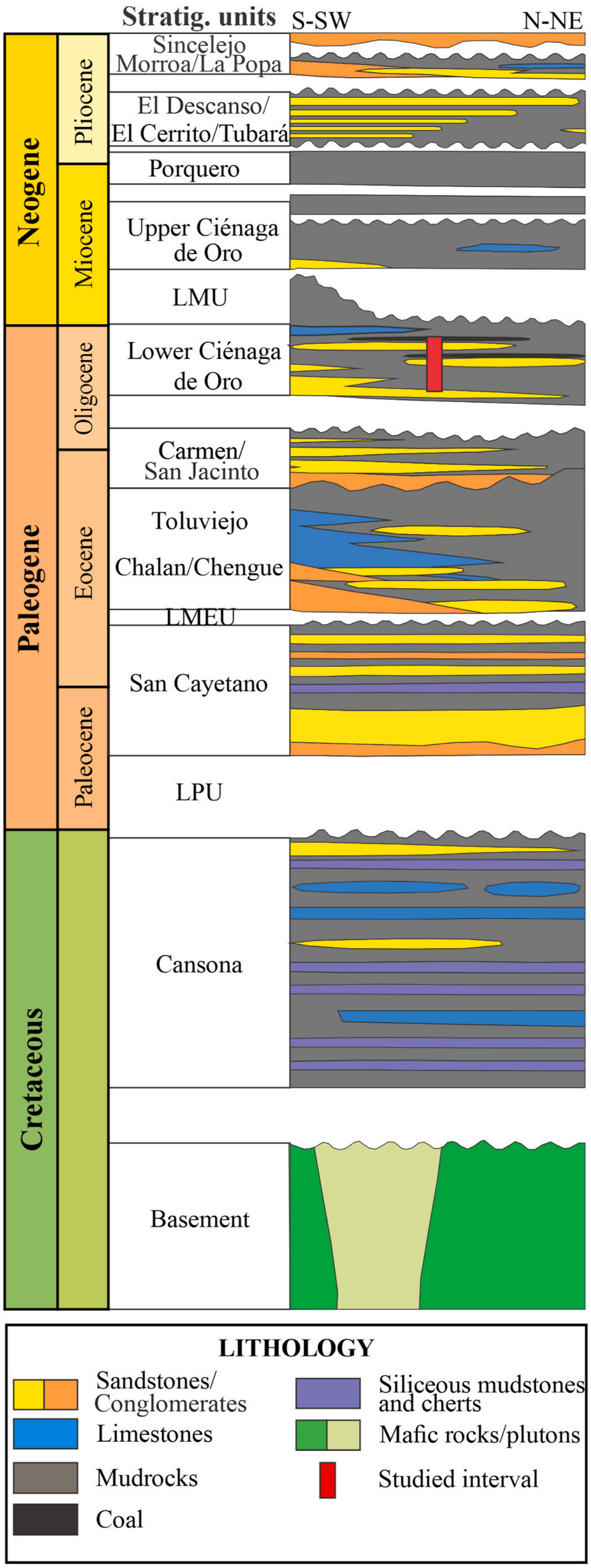

Fig. 2. Schematic chronostratigraphic chart of the Sinú-San Jacinto Basin (modified from Mora et al., 2017, 2018; Osorio-Granada et al., 2020). Note: LPU: lower Paleocene unconformity; LMEU: lower-middle Eocene unconformity; LMU: lower Miocene unconformity.

2.1. *Ciénaga de Oro Formation*

During the Oligocene – early Miocene, thick shallow marine and deltaic deposits accumulated in the southern part of the SSJB corresponding to the Ciénaga de Oro Formation (Dueñas and Duque-Caro, 1981; Dueñas, 1986; Guzmán et al., 2004; Bermúdez et al., 2009; Bermúdez, 2016; Manco– Garc é s et al., 2020). Duque-Caro (1972) in the stratigraphic sections of Arroyo Alférez and Carmen-Zambrano defined the Carmen Group that includes from base to top, Ciénaga de Oro, Porquero and Cerrito formations. Subsequently, Duque-Caro (1973) used the term Ciénaga de Oro to designate the succession of sandstones and mudrocks outcropping on the Montería-Planeta Rica road. The term Ciénaga de Oro Formation is derived from unpublished Intercol oil company reports that use it in the Montería-Planeta Rica and Ciénaga de Oro-La Ye regions (Dueñas and Duque-Caro, 1981). Based on palynological, stratigraphic and seismic studies carried out in the Ciénaga de Oro Formation, an Eocene (?) – Oligocene to lower Miocene age is assigned (Dueñas, 1980, 1983, 1986, 1983; Dueñas and Duque-Caro, 1981; Guzmán et al., 2004; Bermúdez et al., 2009; Mora et al., 2018). The thickness of this unit was measured on the Montería-Planeta Rica road, and corresponds to at least 2500 m of a domain of sandy facies with intercalations of calcareous gray mudrocks, carbonaceous mudrocks and coal (Dueñas and Duque-Caro, 1981).

Dueñas and Duque-Caro (1981) and Mora et al. (2018) divide the Ciénaga de Oro Formation into two segments: lower and upper. The analyzes of planktonic foraminifera in well-cores and outcrops reported by Mora et al. (2018) assign an Oligocene to lower Miocene age for the lower segment. This unit is limited towards the top by a regional unconformity that puts it in contact with the upper segment (Mora et al., 2018), which has a lower to middle Miocene age (Dueñas and Duque Caro, 1981; Mora et al., 2018).

3. Material and methods

In the last years, the National Hydrocarbons Agency (ANH) has drilled several stratigraphic wells in the Colombian Caribbean area in order to characterize the evolution and hydrocarbon potential of the basins. The study succession corresponds to an interval of the ANH-SSJ-Nueva Esperanza-1X stratigraphic well, drilled in the south of the SSJB. The study interval is between 2013 ft–946 ft (~614 m–~288 m) from the top. The well-core was described in detail in the Colombian core repository (Litoteca Nacional-Piedecuesta, Colombia). The Oligocene age data were taken from the biostratigraphic study developed by the Universidad de Caldas for the ANH and Minciencias based mainly on palynomorphs, foraminifera, and calcareous nanofossils (Project Contrato RC 494, 2017) and other previous works in the Ciénaga de Oro Formation (e.g., Dueñas, 1980). A detailed stratigraphic log (scale 1:1) was carried out taking into account the lithology (texture, composition), sedimentary structures, contact types, and paleontological contents (fossils, and biogenic sedimentary structures). The thicknesses of the beds are described following the nomenclature of Nichols (2009): very thin beds (<1 cm), thin beds (1–10 cm), medium beds (10–30 cm), thick beds (30–100 cm), very thick beds (>100 cm). Special attention was paid to the detailed ichnological characterization, including ichnological features such as size of trace fossils, type of fill, orientation, relationship with the facies and stratigraphic surfaces, and tiering, as well as ichnodiversity, distribution and abundance (Bioturbation Index, BI, sensu Taylor and Goldring, 1993) of the structures. Ichnotaxonomical assignation is based on the recognition of ichnotaxobases as observed in cores (Knaust, 2017). The facies codes were assigned from the terminology used by Collinson and Mountney (2019).

4. Sedimentology and ichnology

4.1. Facies

The well-core segment studied corresponds to a siliciclastic succession approximately 1069 ft (~326 m) thick. Five lithological groups were differentiated in the study succession (sandstones - Fig. 3, mudrocks - Fig. 4, conglomerates - Figs. 3–4, bioclastic sediments - Figs. 3–4, and coal levels - Fig. 4), as well as the definition of sedimentary facies (Table 1; Figs. 3 and 4).

The study interval is formed mainly by thin, medium and thick sandstone beds from very fine-medium to coarse-slightly conglomeratic sizes, gray and yellowish gray. Also, the grain-selection is variable from poor to well sorted. Internally and throughout the well-core, massive

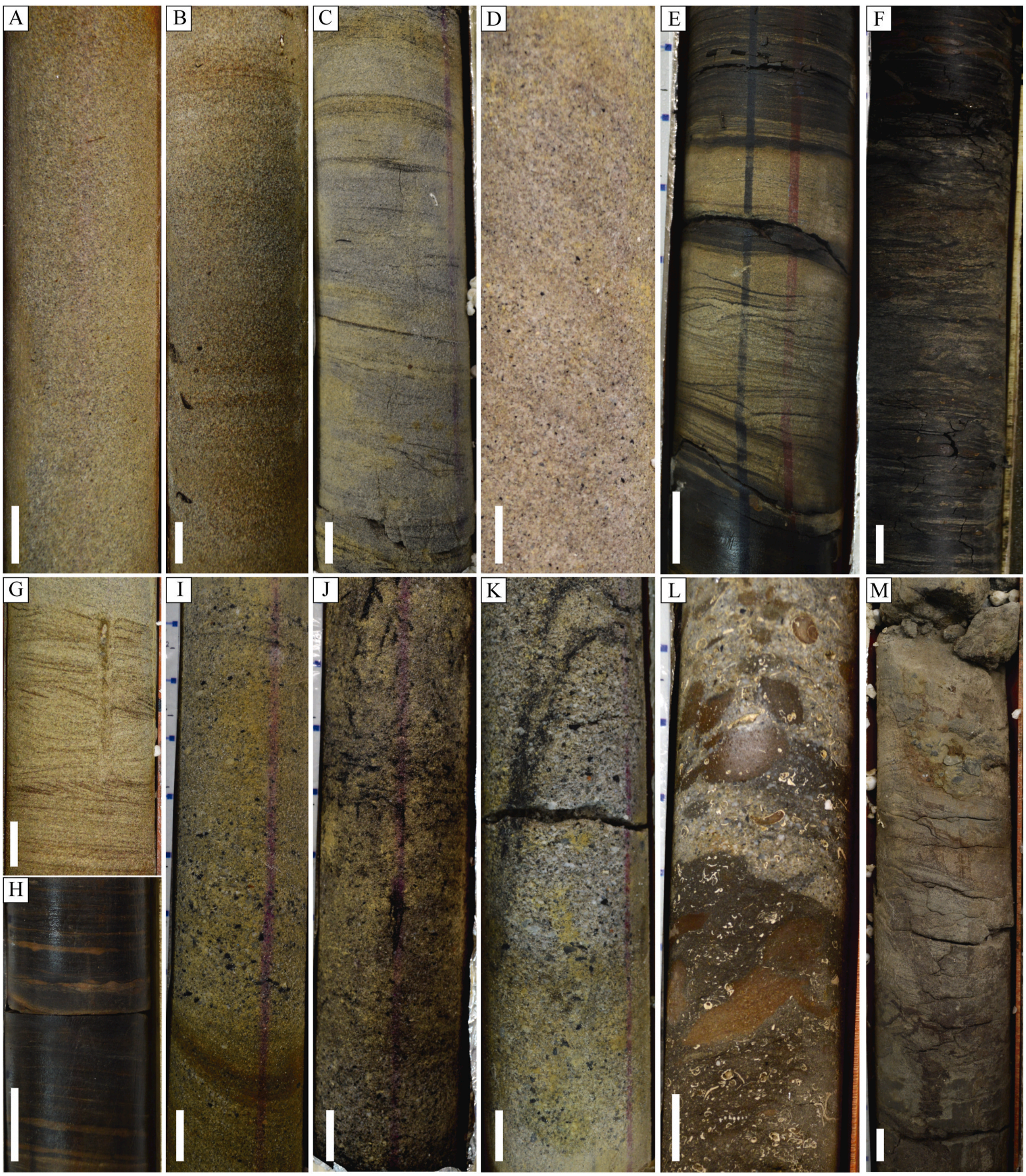

Fig. 3. Main sedimentary structures identified in the sandstones of the study succession. Scale bar: 2 cm. In parentheses, location of the photograph in the well (feet - meters from the top). **A.** Massive sandstone (Sm; 1506 ft - ~459 m). **B.** Horizontal lamination sandstone (Sh; 1053 ft - ~321 m). **C.** Low angle cross-bedding sandstone (Sa; 1884 ft - ~574 m). **D.** Planar cross-bedding sandstone (Sp; 1089 ft - ~332 m). **E.** Hummocky cross-stratification (HCS; 1895 ft - ~578 m); **F.** Convolute lamination sandstone (Sc; 1935 ft - ~590 m). **G.** Asymmetrical ripples in sandstone (Sr; 1681 ft - ~512 m). **H.** Symmetrical ripples in sandstone (Sw), and load casts (Slc; 1948 ft - ~594 m). **I.** Trough cross-bedding sandstone (St; 1783 ft - ~543 m). **J.** Normal gradation of coarse-grained sandstone to medium fine-grained sandstone (Sng; 1776 ft - ~541 m). **K.** Inverse gradation of medium-grained sandstone to coarse-grained sandstone (Sig; 1619 ft - ~493 m). **L.** Massive bioclastic sandstone (Sb; 1153 ft - ~351 m). **M.** Load casts (Slc; 1092 ft - ~333 m).

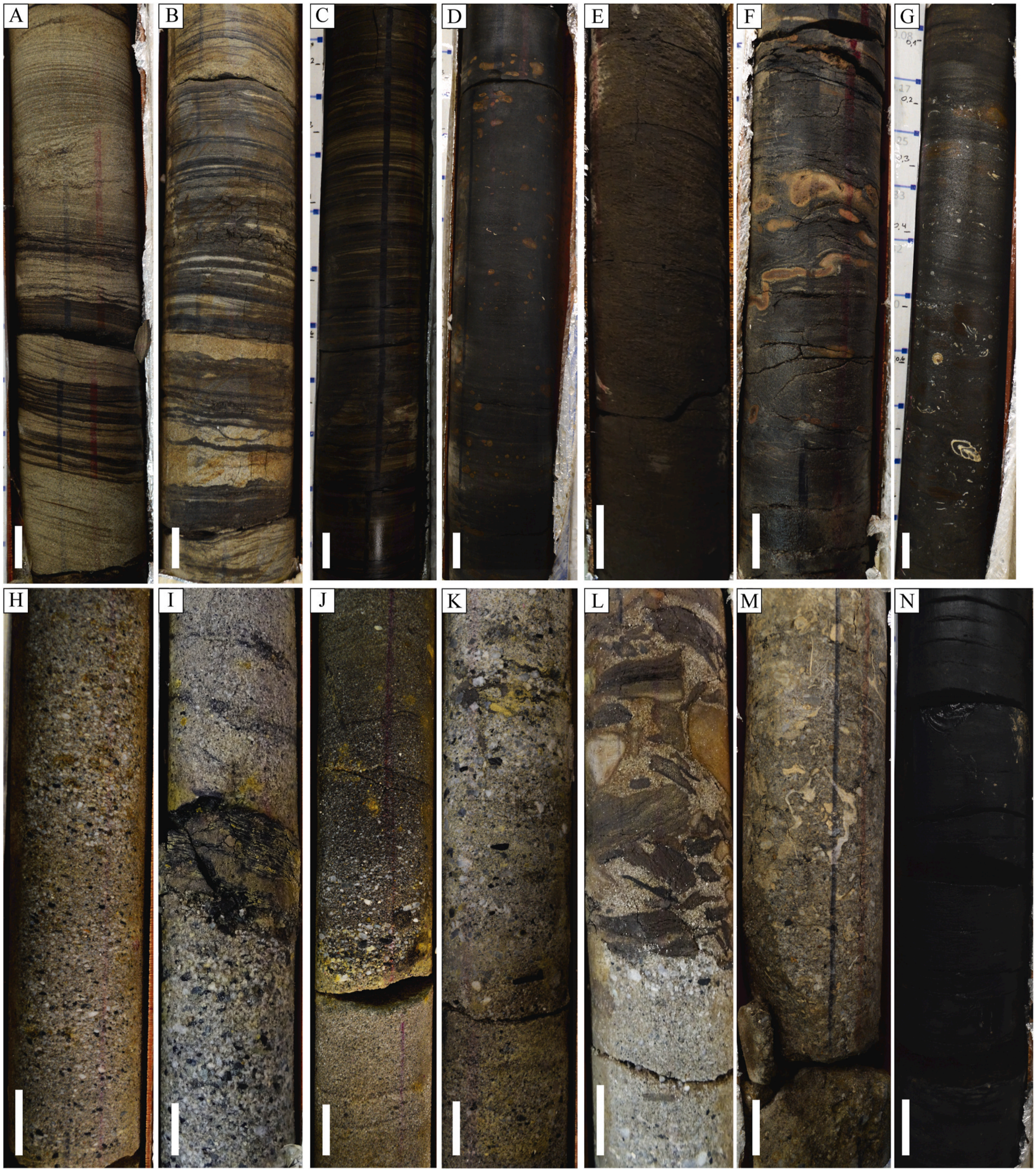

Fig. 4. Main sedimentary structures identified in the sandstones and mudrock interbedded, mudrocks, conglomerates, and coal beds of the study succession. Scale bar: 2 cm. In parentheses, location of the photograph in the well (feet - meters from the top). **A.** Flaser bedding (Htf; 1894 ft - ~577 m). **B.** Wavy bedding (Htw; 1299 ft - ~396 m). **C.** Lenticular bedding (Htl; 1934 ft - ~589 m). **D.** Massive mudrock (Mm; 1916 ft - ~584 m). **E.** Horizontal lamination mudrock (Mh; 999 ft - ~304 m); **F.** Syneresis cracks (Ms; 1397 ft - ~426 m). **G.** Massive bioclastic mudrock (Mb; 1923 ft - ~586 m). **H.** Massive polymictic matrix-supported conglomerates (Gmm; 1586 ft - ~483 m). **I.** Massive polymictic clast-supported conglomerates (Gcm; 971 ft - ~296 m). **J.** Normal gradation of granule-sized conglomerate to medium-grained sandstones (Gng; 1583 ft - ~482 m). **K.** Inverse gradation of medium coarse-grained sandstone to granule-sized conglomerate (Gig; 1191 ft - ~363 m). **L.** Massive oligomictic clast-supported conglomerates (Goc; 965 ft - ~294 m). **M.** Massive bioclastic conglomerate (Gb; 1980 ft - ~603 m). **N.** Massive coal (Co; 1842 ft - ~561 m).

structure (Sm; Fig. 3A), horizontal lamination (Sh; Fig. 3B), low-angle cross-bedding (Sa; Fig. 3C), planar cross-bedding (Sp; Fig. 3D), and trough cross-bedding are present (St; Table 1; Figs. 3I and 5). Sandstones and mudrocks intercalations are observed, showing flaser (Htf; Fig. 4A), wavy (Htw; Fig. 4B) and lenticular bedding (Htl; Fig. 4C), where the occurrence of mud-drapes is also common (Table 1; Fig. 5). In addition, in some intervals hummocky cross-stratification (HCS; Fig. 3E) is observed, as well as convolute lamination (Sc) (Fig. 3F), flame structure, load casts (Sf, Slc; Fig. 3H-M), and asymmetrical (Sr; Fig. 3G) and symmetrical ripples (Sw; Fig. 3H; Table 1; Fig. 5). Some massive sandstones (Sm) have rhizoliths. In some intervals, there are medium-to coarse-grained sandstones with fragments of organic matter, erosive bases and tops with normal gradation (Sng; Fig. 3J) to fine and very fine-grained sandstones. Occasionally, inverse gradation (Sig; Fig. 3K) to

Table 1
Sedimentary facies and hydrodynamic interpretation.

Lithological group	Sedimentary structure	Facies Code	Hydrodynamic processes	References
Sandstones	Massive structure	Sm	Rapid deposition, most probably through the deceleration of a heavily sediment-laden current. Destruction of depositional lamination can come about through intense reworking of sediment.	Collinson et al. (2006), Collinson and Mountney (2019)
	Horizontal lamination	Sh	High velocity currents, probably associated with upper flow regime in fine- to medium-grained sandstones and that it is not very micaceous.	Collinson and Mountney (2019), Heldreich et al. (2017)
	Low-angle cross-bedding	Sa	Washed-out dunes that occur between subcritical flow regimes. Deposited by traction from relatively weak currents that approach upper flow regime conditions for the size of sediment being deposited.	Picard and High (1973), Heldreich et al. (2017)
	Planar cross-bedding	Sp	Unidirectional migration of 2D straight-crested ripples and thalweg bars in high-energy fluvial channels, under lower flow regime.	Heldreich et al. (2017), Collinson and Mountney (2019)
	Hummocky cross-stratification	HCS	Deposition during high-energy oscillatory or combined flows. Strong and complex wave activity, mainly in areas below fair-weather wave base.	Collinson and Mountney (2019)
	Convolute lamination	Sc	Plastic deformation of partially liquefied sediment, usually occurring soon after deposition.	Collinson and Mountney (2019)
	Asymmetrical ripples	Sr	Result from currents flowing in one direction only (unidirectional).	Collinson and Mountney (2019)
	Symmetrical ripples	Sw	Bidirectional, oscillatory wave motion creates straight-crested symmetrical wave ripples. Represents deposition under wave action or in shallow water with stable flow conditions.	Heldreich et al. (2017), Collinson and Mountney (2019)
	Trough cross-bedding	St	Produced during unidirectional migration of sinuous to linguoid-crested ripples or dunes (depending of the scale) in high to moderate energy.	Collinson and Mountney (2019)
	Normal gradation (Medium- to coarse- grained sandstones to fine and very fine-grained sandstones)	Sng	This suggests a decelerating current from suspension of sediments, with coarsest particles falling to the bed first.	Collinson and Mountney (2019)
Sandstones and conglomerates	Inverse gradation (Medium- to coarse- grained sandstones to conglomeratic sandstones and granule-sized matrix-supported conglomerate)	Sig	Dispersive pressure caused by mutual impacts of grains behaving inertially within a rapidly shearing layer.	Reading (1996), Hand (1997), Collinson et al. (2006)
Bioclastic sandstones	Massive bioclastic sandstones	Sb	Rapid deposition, most probably through the deceleration of a heavily sediment-laden current. Destruction of depositional lamination can come about through intense reworking of sediment.	Collinson et al. (2006)
Sandstones and mudrocks	Load casts and flame structures	Slc, Sf	Differences in density between the beds.	Collinson and Mountney (2019)
	Flaser bedding Wavy bedding Lenticular bedding	Htf Htw Htl	Water movement over a sand bed, as unidirectional currents, oscillatory waves or combination of both. The variation in mud and sand content is the result of increasing/decreasing in current speed.	Collinson et al. (2006).
Mudrocks	Massive	Mm	Vertical settling by weak suspension currents, intense bioturbation, high viscosity sediment - water flows under low energy conditions or in standing bodies of water (mudflows).	Shanmugam (1997), Potter et al. (2005)
	Horizontal lamination	Mh	Vertical settling by weak suspension currents in very low energy conditions.	Potter et al. (2005)
	Syneresis cracks	Ms	They are produced by the expulsion of liquid that generates the spontaneous contraction experienced by a recently deposited clay, in contact with a saline solution. This subaqueous shrinkage in argillaceous sediments can also be caused by earthquake-induced dewatering.	Astin and Rogers (1991), Pratt (1998), Tanner (2003)
Bioclastic mudrocks	Massive bioclastic mudrocks	Mb	Vertical settling by weak suspension currents, intense bioturbation, dense mudflows along the bottom.	Shanmugam (1997), Potter et al. (2005)
Conglomerates	Massive polymictic matrix-supported	Gmm	Transport and deposition of such hyper-concentrated sediments occur in high-energy flow conditions.	Collinson and Mountney (2019)
	Massive polymictic clast-supported	Gcm	Transport and deposition of such hyper-concentrated sediments occur in high-energy flow conditions.	Collinson and Mountney (2019)
	Normal gradation (Granule-sized and a lesser extent, pebble matrix-supported conglomerates to medium- to coarse- grained sandstones)	Gng	Deceleration of the flow with coarsest particles falling to the bed first.	Lowe (1976), Collinson and Mountney (2019)
	Inverse gradation (Medium- to coarse- grained sandstones to conglomeratic sandstones and granule-sized matrix-supported conglomerate)	Gig	Dispersive pressures operated, the density-modified grain flow. Inverse grading may also result from growth of low-relief bars though a clast-supported fabric is then more likely.	Todd (1989), Nemec and Postma (1993)
	Massive oligomictic clast-supported	Goc	Transport and deposition of such sediments occur in high-energy, but some of the clasts originated from within the basin of deposition and were eroded from penecontemporaneous sediments.	Collinson and Mountney (2019)
Bioclastic conglomerates	Massive bioclastic conglomerates	Gb	Rapid deposition, most probably through the deceleration of a heavily sediment-laden current. Destruction of depositional lamination can come about through intense reworking of sediment.	Collinson et al. (2006)
Coal	Massive coal	Co	Calm hydrodynamic conditions that allow the preservation of organic matter suggests low oxygen conditions.	Collinson and Mountney (2019)

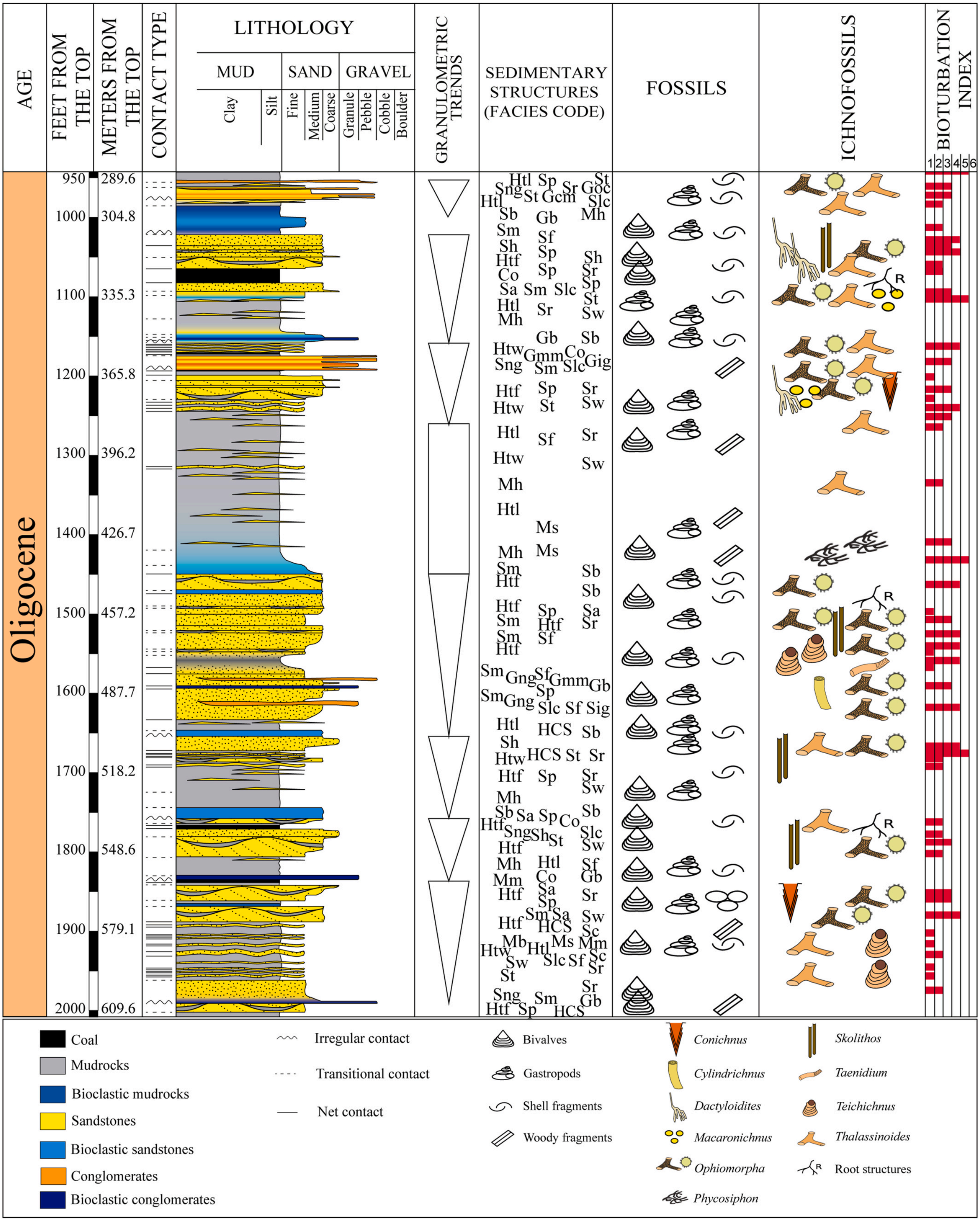

Fig. 5. Stratigraphic log of the studied interval (scale 1:2000), including sedimentological (lithology, contact type, grain size, sedimentary structures-facies) and paleontological (fossils, ichnofossils and Bioturbation Index) features. For facies codes see Table 1.

conglomeratic sandstones and granule-sized matrix-supported conglomerates, and then normal gradation to coarse and medium-grained sandstones is registered (Table 1; Fig. 5). Bioturbation index in sandstones range from 0 to 5. Massive sandstones (Sm) generally exhibit the highest values of BI = 4–5 (Table 1; Fig. 5).

Thin, medium and thick light gray to dark/black mudrock beds are common in the study succession (Table 1; Fig. 5). They occur mainly with lenticular bedding (Htl; Fig. 4C) and, occasionally, massive structure (Mm; Fig. 4D), and horizontal lamination (Mh; Fig. 4E), with a variable but low bioturbation index (BI = 0 and 2; Table 1; Fig. 5). Some syneresis cracks (Ms; Fig. 4F), iron and siderite nodules and, occasionally, accompanied by rhizoliths are also observed (Table 1; Fig. 5). The micropaleontological analysis reveals the presence of mudrocks levels with few calcareous nanofossils, foraminifera (benthic and planktonic), and marine palynomorphs (dinoflagellates), and in a higher proportion pollen and spores (Project Contrato RC 494, 2017).

Throughout the study interval, thin, medium and thick beds of gray and yellowish gray polymictic granule-sized matrix- and clast-supported conglomerates (Gmm, Gcm; Fig. 4H and I) associated with sandstones. To a lesser extent, pebbles-sized conglomerates are observed (Table 1; Fig. 5). Their clasts are subangular to subrounded, moderately to well sorted. Change to sandstones beds can be gradational (Gng, Gig; Fig. 4J and K), erosive or net (Table 1; Fig. 5). Rarely, pebble-sized oligomictic clast-supported conglomerates (Goc; Fig. 4L) are observed consisting of mudrocks clasts (Table 1; Fig. 5). Woody fragments are also common. Biogenic sedimentary structures in the conglomerates are scarce, although in the variations from medium to coarse sandstones to conglomeratic sandstones and to granule-sized matrix-supported conglomerates, traces of *Ophiomorpha* and bioturbation index between 0 and 2 are observed (Table 1; Fig. 5).

Frequently, medium to thick bioclastic sandstones beds (Sb; Fig. 3L) with indeterminate shell fragments, bivalves and gastropods fragments occur (Table 1; Fig. 5). They show slight variations to granule-sized bioclastic matrix-supported conglomerates (Gb; Table 1; Fig. 4M; Fig. 5). Thin and medium bioclastic mudrock beds (Mb) with slight variations to bioclastic sandstones (Sb; Fig. 4G) are also locally recognized, with, bivalves, and gastropods and indeterminate shell fragments (Table 1; Fig. 5). On some occasions, granule-sized bioclastic matrix-supported conglomerates (Gb; Fig. 4M) are observed in net contact on the sandstones or medium coal beds (Co; Table 1; Fig. 5). The bioclastic content of the conglomerates consists of indeterminate shell fragments, as well as bivalves and gastropods. Bioturbation index in bioclastic sediments range from 0 to 2.

Very thin, thin, and medium coal beds (Co; Fig. 4N) are also observed in the study interval (Fig. 4), with a variable relationship with the other lithologies (Table 1; Fig. 5). The base usually presents net contacts with other lithologies and occasionally transitional contacts from carbonaceous mudrocks. The top of these coal beds shows transitional change to mudrocks, and/or erosive contacts with bioclastic sediments (bioclastic sandstones (Sb) and/or bioclastic conglomerates (Gb)), and to a lesser extent to massive sandstones (Sm; Table 1; Fig. 5). Bioturbation index 3–4 characterize the top of some of these coal beds (Table 1; Fig. 5).

4.2. Trace fossils

Trace fossil assemblage in the studied succession is low abundant and moderately diverse. Ten ichnogenera have been recognized, including *Conichnus*, *Cylindrichnus*, *Dactyloidites*, *Macaronichnus*, *Ophiomorpha*, *Phycosiphon, Skolithos*, *Taenidium*, *Teichichnus*, *Thalassinoides*, as well as undifferentiated rhizoliths. The bioturbation index ranges from 0 (no traces) to 4–5 (intense bioturbation to almost completely disturbed bedding). In numerous intervals *Ophiomorpha* is the only trace fossil present. In other cases, *Conichnus*, *Cylindrichnus*, *Dactyloidites*, *Macaronichnus*, *Phycosiphon*, *Skolithos*, *Taenidium*, *Teichichnus*, and *Thalassinoides* are also registered as exclusive traces. Furthermore, the associations *Ophiomorpha-Conichnus*, *Ophiomorpha-Thalassinoides*, *Conichnus-Dactyloidites-Ophiomorpha* are recognized.

Conichnus (Fig. 6A), is a relatively large conical burrow with subcircular cross section and subvertical orientation. The passive filling may include a thin lining along the wall of the burrow (Frey and Howard, 1981). Internally, *Conichnus* often show downward deviated blades determining a chevron appearance, primarily in response to the vertical adjustment of the producer (Knaust, 2017). The recognized specimens have approximately a cross section ~8 cm long and ~2 cm wide. The thin lining along the wall of the burrow is observed, as well as the deviation of the sediment sheets downwards (Fig. 6A). Specimens are found in medium-grained sandstones with incipient horizontal lamination (Sh), and massive sandstones (Sm), sometimes together with *Ophiomorpha* (Fig. 6A). *Conichnus* is a common element of shallow marine and, nearshore environments where occur high-energy sedimentary processes, high sediment supply, and frequently mobilized substrate (e.g., Abad et al., 2006). It also occurs in shallow intertidal to subtidal environments, and can be associated with wave structures, dunes and megaripples (e.g., Savrda, 2002).

Cylindrichnus (Fig. 6B), includes arc-shaped or U-shaped burrows with a passive fill and a concentric laminated lining (Ekdale and Harding, 2015). They are usually unbranched, although branching has been documented (Knaust, 2017). Observed *Cylindrichnus* burrows have subvertical shapes with a slight arc shape with sizes between ~4 and 6 cm long, and ~1 cm wide. Displaying the diagnostic thick lining highlighted by sheets of organic matter enclosing a thin central to eccentric tube (Fig. 6B). This trace fossil is found mainly in massive medium-to fine-grained sandstones with a high content of organic matter (Sm). *Cylindrichnus* is characteristic of high-energy deposits, including storm deposits, sand dunes, and sandbanks, where vertical forms predominate (e.g., Howard, 1966; Pemberton and Frey, 1984; Frey, 1990; Knaust, 2017). It is a common component of marine and estuarine environments with brackish conditions (e.g., Netto and Rossetti, 2003; MacEachern and Gingras, 2007; Buatois and Mángano, 2011; Gingras and MacEachern, 2012) and occurs in association with delta front and prodelta deposits (e.g., Tonkin, 2012). In addition, this trace fossil has been frequently reported in moderate to low energy deposits from the shelf to the lower shoreface where horizontal morphologies predominate (e.g., Fü rsich, 1974; Belaústegui and de Gibert, 2013).

Dactyloidites (Fig. 6C) is a fan-shaped rosette trace formed by radial elements and a vertical central tube. The radial elements, sub-horizontal or inclined with respect to the bedding plane, arise from the vertical tube, and present protrusive connections (spreite) generated by the downward movement of the tube (Fürsich and Bromley, 1985). Radial elements can be sub-horizontal or inclined with respect to the bedding plane (Fürsich and Bromley, 1985). In the study succession, *Dactyloidites* is locally recognized as circular to subcircular sections, occasionally elongated, associated with the terminations of the rosette with a better selected filling and with a lighter coloration than the host rock (Fig. 6C). They have average diameters of ~0.5 cm and appear isolated and/or grouped, but no overlap is observed. Sometimes it appears as an exclusive trace or associated with *Ophiomorpha* and always into massive medium-to fine-grained sandstones (Sm), or low angle cross-bedding medium-to fine-grained sandstones (Sa) or horizontal lamination medium-to fine-grained sandstones (Sh) (Fig. 6C). Observed specimens show similarities with those described in cores by de Gibert et al. (1995). However, given that the vertical central tube is not observed in the study specimens, its assignment to the ichnogenus is tentative ?*Dactyloidites*. This ichnogenus is common in high energy shallow marine environments, and usually present in conditions of warm climates (de Gibert et al., 1995). Furthermore, it has been described in fluvial-dominated deltas (Gilbert type and mouth bar type; Agirrezabala and de Gibert, 2004), in environments with a high contribution of organic debris (e.g., Boyd and McIlroy, 2016), and in lower shorefaces influenced by storms (e.g., Lazo et al., 2008). Particularly are associated with sediments in the last stages of sedimentary courtship at high sea level (highstand system tract; Uchman and Pervesler, 2007).

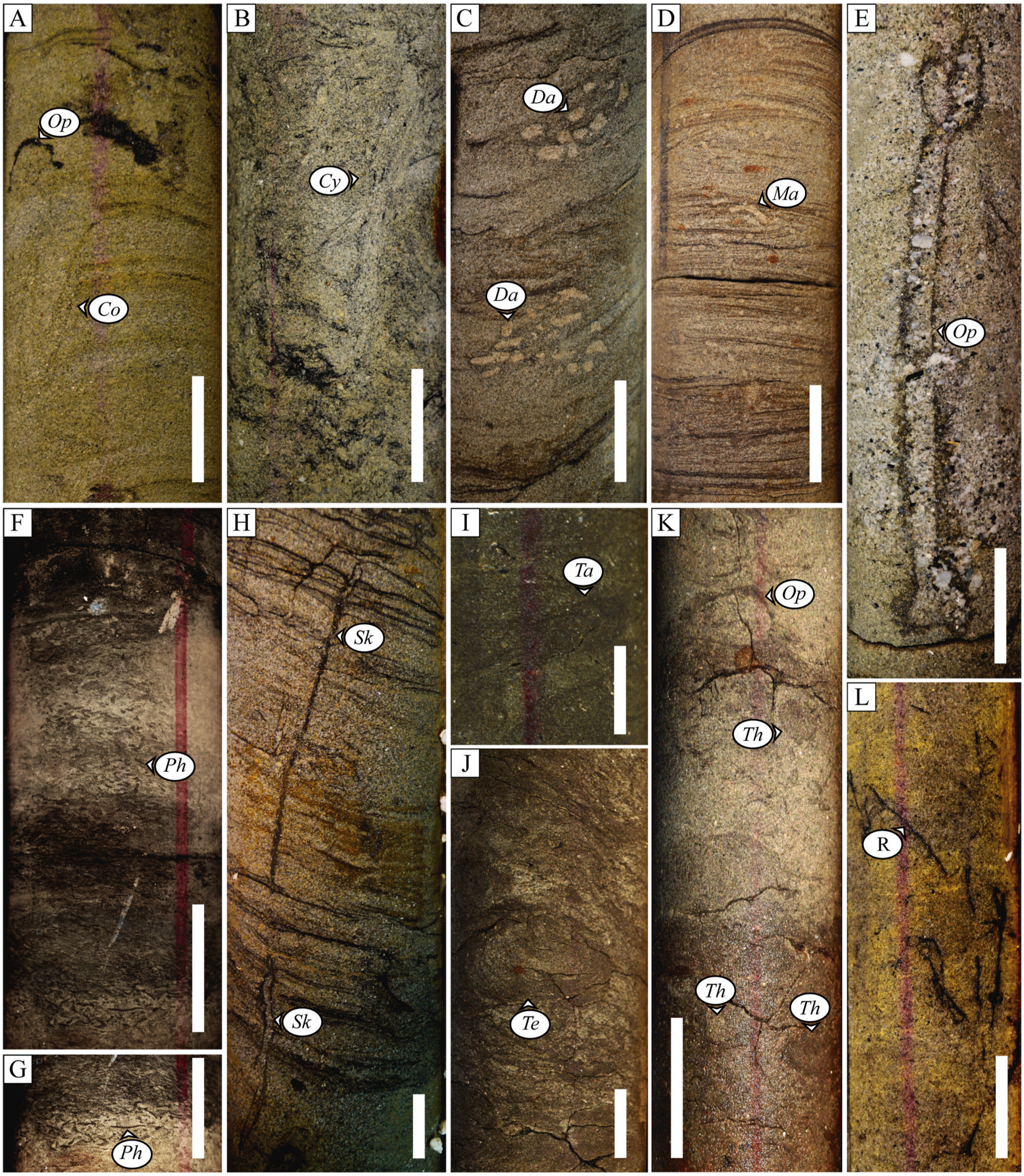

Fig. 6. Ichnogenus and rhizoliths recognized in the study succession. **A.** *Conichnus* (*Co*) and *Ophiomorpha* (*Op*) (1875 ft - ~572 m). **B.** *Cylindrichnus* (*Cy*) (1608 ft - ~490 m). **C.** *Dactyloidites* (*Da*) (1045 ft - ~319 m). **D.** *Macaronichnus* (*Ma*) (1231 ft - ~375 m). **E.** *Ophiomorpha* (*Op*) (1186 ft - ~361 m). **F - G.** *Phycosiphon* (*Ph*) (1438 ft - ~438 m). **H.** *Skolithos* (*Sk*) (1043.5 ft - ~318 m). **I.** *Taenidium* (*Ta*) (1578 ft - ~481 m). **J.** *Teichichnus* (*Te*) (1551 ft - ~472,7 m). **K.** *Ophiomorpha* (*Op*) and *Thalassinoides* (*Th*) (1541 ft - ~470 m). **L.** Rhizoliths (R) (1775 ft - ~541 m). Scale bar: 3 cm. In parentheses, location of photograph in well (feet - meters).

Macaronichnus (Fig. 6D) includes predominantly horizontal, cylindrical burrows, with a straight, sinuous, meandering or spiral-shaped morphology, although oblique and vertical forms can also occur (Clifton and Thompson, 1978; Knaust, 2017). Burrows are characterized by an active fill of sand lighter than that of the embedded sediment and a rim composed of dark mineral grains (mica or heavy minerals) that commonly occur in high density (Clifton and Thompson, 1978; Knaust, 2017). Here *Macaronichnus* is scarce (2 intervals), consisting of cylindrical burrows with elongated, elliptical and circular sections (Fig. 6D). The diameter ranges from 0.1 cm to 0.4 cm and its length can be at least 2 cm. The burrow fill contrasts with the surrounding sediment by its pale colour, and the halo of dark minerals is recognizable. It is registered either as some scattered specimens (Fig. 6D) or with a high density in a completely bioturbated interval (~1 m), in massive medium-to fine-grained sandstones (Sm), flaser bedding (Htf), or fine sandstones with planar cross-bedding (Sp), and horizontal lamination (Sh). *Macaronichnus* is typically associated with sandy unconsolidated substrates (Knaust, 2017). *M. segregatis* is a shallow marine trace, very common in beach, shoreface, and delta front deposits, as well as in shallow intertidal and subtidal deposits (e.g., Nara and Seike, 2004; Seike, 2007; Bromley et al., 2009; Quiroz et al., 2010, 2019; Uchman et al., 2016). *M. segregatis degiberti* is also occasionally recorded in deeper environments (e.g., Rodrí guez – Tovar and Aguirre, 2014; Knaust, 2017; Giannetti et al., 2018; Miguez– Salas et al., 2020; Dorador et al., 2021).

Ophiomorpha (Fig. 6A-E-K), consists of burrows showing a horizontal frame with vertical axes, and circular to elliptical in cross section. The branch is Y- and T-shaped, typically with enlargement of the junctions. Passive filling is common, although some segments of the burrow may have a meniscal filling (Knaust, 2017). Burrow lining is diagnostic of *Ophiomorpha*, consisting of sand and/or mud granules along the wall or pellets (Frey et al., 1978). *Ophiomorpha* is abundant in the studied succession, both as an exclusive trace or associated with other ones (Fig. 6A–K). It is recorded in massive sandstones (Sm), massive conglomeratic sandstones (Sm; Fig. 6E), and massive polymictic matrix-supported granule-sized conglomerates (Gmm; Fig. 6E). The diameter of the burrows varies between ~0.5 cm and ~3 cm, and the longitudinal sections between ~3 cm and ~12 cm (Fig. 6E). The presence of pellets in the wall is characteristic in all the observed specimens. *Ophiomorpha* is found in a wide variety of paleoenvironments, being, although not exclusively, a typical component of high-energy environments. Originally considered as a significant element of shallow marine facies (Frey et al., 1978; Pollard et al., 1993), various ichnospecies of *Ophiomorpha* are also characteristic of deep-sea deposits (Uchman, 2009), and their relationship in different facies is discussed (Monaco et al., 2009). Occasionally, *Ophiomorpha* is documented in continental environments, mainly in Permian sediments associated with the first records of crustaceans (e.g., Baucon et al., 2014), although these burrows can also be produced by other organisms and assigned to different ichnotaxa (Goldring and Pollard, 1995).

Phycosiphon (Fig. 6F and G) is a small burrow consisting of repeated narrow U-shaped, or hooked lobes, each of which encloses a spreite of millimeter to centimeter scale and branches regularly or irregularly from an axial spreite of similar width (Wetzel and Bromley, 1994). The study specimens have been recognized in a 60 cm-thick interval of massive muddy sediments (Mm) with slight variations to massive very fine sandstones (Sm), distributed in patches, showing various lobe orientations, resulting in a chaotic arrangement. Burrow length varies between ~0.1 cm and ~0.5 cm and rarely reach 1 cm (Fig. 6F and G). *Phycosiphon* is a characteristic component of offshore-platform to lower shoreface deposits, commonly occurring as exclusive trace or in higher ichnodiversity siliciclastic successions (Goldring et al., 1991), as well as in deltaic environments (e.g., Rodrí guez – Tovar et al., 2014). It also occurs in slope deposits (e.g., Naruse and Nifuku, 2008), and is common in deep marine environments (e.g., Celis et al., 2018). *Phycosiphon* producers are among the first bioturbators of event deposits such as storms, turbidity currents, and bottom current (e.g., Goldring et al., 1991; Wetzel, 2008; Rodrí guez – Tovar et al., 2014).

Skolithos (Fig. 6H) consist of a subvertical cylindrical tube with or without a liner, and passive filling (Alpert, 1974). A funnel-shaped opening can be developed or preserved at the top (Knaust, 2017). Throughout the study succession, *Skolithos* specimens correspond to vertical/subvertical straight lined burrows, arranged perpendicular to the horizontal lamination of fine-to medium-grained sandstones (Sh). Longitudinal section generally has a millimeter thickness (~0.2 cm on average) and a length between ~4 cm and ~10 cm (Fig. 6H). They are also observed in massive medium-to fine-grained sandstones (Sm), and flaser bedding (Htf). *Skolithos* is a common indicator of relatively high energy, shallow water, and nearshore to marginal marine environments (Knaust, 2017). However, some authors record it as a common component of fluvial and other continental deposits (e.g., Hasiotis, 2010).

Taenidium (Fig. 6I) is a meniscate cylindrical burrow, predominantly sub-horizontal but can also be subvertical. Burrows have not lining or it is very thin and they are not branched (D' Alessandro and Bromley, 1987). The meniscate filling is usually widely spaced with little contrast in lithology (D' Alessandro and Bromley, 1987). Observed specimens occur in sandy-silty and sandy sediment (Sm), as sub-horizontal (Sa) or inclined (~45°) structures (Sp), respectively, diameter of ~1 cm and variable presence of meniscus (Fig. 6I). *Taenidium* has been recorded from a wide variety of environments. It is commonly found in marginal alluvial, fluvial and lake environments (Savrda et al., 2000; Hasiotis, 2010; Melchor et al., 2012). *Taenidium* is also of special interest, particularly in the transition zone between terrestrial and terrestrial aquatic environments (e.g., Rodrí guez – Tovar et al., 2016). It is also common in transitional environments (e.g., fluvial-tidal transition; Dí ez – Canseco et al., 2015), but it also belongs to the *Cruziana* ichnofacies in the offshore zone. *Taenidium* is also in shallow and deep marine deposits (e.g., D' Alessandro and Bromley, 1987; Miguez– Salas and Rodr í guez – Tovar, 2019). Recently *Taenidium*, has been registered linked to hyperpycnal systems (García-García et al., 2021).

Teichichnus (Fig. 6J) is a spreite burrow with a subvertical wall and a straight or curved plan arrangement containing stacked lamellae and a causative burrow with passive fill (Knaust, 2018). In vertical sections *Teichichnus* usually appear as groups of vertical to highly inclined spreiten, which can pile up one on top of the other due to different sedimentation events (Knaust, 2017). In the studied section *Teichichnus* is observed showing a subvertical disposition, where the spreite is easily recognized due to the contrast with the hosting sediment that varies between massive siltstone (Mm) and very fine sandstone (Sm). They are ~1 cm wide, and ~3 cm long (Fig. 6J). *Teichichnus* is typically in siliciclastic systems, occurring frequently into deltaic deposits (e.g., Tonkin, 2012). Its producers can be considered as euryhaline organisms capable of adapting to a wide range of salinity; it has often been recognized in reduced salinity settings (Knaust, 2018). Such conditions are common in marginal marine environments (e.g., inlets-bays, estuaries, lagoons), where *Teichichnus* is widespread (Knaust, 2017). Furthermore, it is frequently present in tidal deposits including dunes and bars in brackish environments (Desjardins et al., 2012) and hyperpycnal flow deposits (e.g., Buatois et al., 2011). In contrast to such marginal marine occurrences with low ichnodiversity, *Teichichnus* is characteristic of lower shoreface to offshore-platform deposits, in high diverse assemblages (Knaust, 2018). *Teichichnus* has been used in sequence stratigraphy analysis as an indicator of flood events, being characteristic of transgressive system tracts (Pemberton et al., 1992; Taylor et al., 2003).

Thalassinoides (Fig. 6K) consists of burrows horizontal, variable, frames with vertical axes, similar to *Ophiomorpha* (Knaust, 2017). Burrows are circular to elliptical in cross section, unlined, and branching is Y- and T-shaped, typically with bulbous enlargement of the junctions (Knaust, 2017). Passive filling is common, although burrow elements can be actively filled (Knaust, 2017). *Thalassinoides* is abundant throughout the studied section, as circular and elliptical cross-sections, with an average diameter ~1 cm (Fig. 6K) and, occasionally, with vertical axes. The passive fill, mainly sandy, in most cases contrasts with the embedded sediment. They are recorded in coal levels (Co), and in massive sandstones (Sm). *Thalassinoides* are more common in shallow marine environments such as shoreface, and deltas (Knaust, 2017), but it is found in a wide range of marine environments, from marginal to deep (e.g., Rodrí guez – Tovar et al., 2008; Rodrí guez – Tovar et al., 2017; Monaco et al., 2009). Given the producer can tolerate fluctuations in salinity, *Thalassinoides* can be found in brackish environments (e.g., estuaries and delta fans) (Knaust, 2017). *Thalassinoides* is often associated with firm substrates, associated with the *Glossifungites* ichnofacies (MacEachern et al., 2007b).

Rhizoliths (Fig. 6L). Root structures found in the study succession range in diameter from ~1 mm to ~10 cm. They have irregularly distributed, and unbranched. Their fill is carbonaceous, sandy, or sand-filled with a thin carbonaceous lining (Fig. 6L). They occur mainly in massive sandstones (Sm; Fig. 6L), and massive clayey siltstones (Mm). Plants commonly colonize terrestrial and aquatic environments in continental settings, such as alluvial, fluvial, lacustrine, and aeolian deposits (e.g., Hasiotis, 2010; Knaust, 2015, 2017; see recent review in Esperante et al., 2021). Mangroves deposits and other rooted deposits are also found in marginal marine environments, including swamps, lagoons, and tidal flats (e.g., Whybrow and McClure, 1980; Knaust, 2009). Transitional zones (marine to continental sequences) that present rhizoliths indicate subaerial exposure (Husinec and Read, 2011; Knaust, 2017).

4.3. Distribution of facies and trace fossils

4.3.1. Study interval

Throughout the study interval, we recognized seven repetitive successions of different thickness, showing slight variations, but being common the upward increase in grain size (coarsening upward trend), as well as the upward decrease in trace fossils diversity, shell fragments (Fig. 5) and marine calcareous microfossils. The successions have thicknesses from ~50 ft (~15 m) to ~160 ft (~49 m), and a succession in the intermediate part of the study interval, which presents a thickness of ~285 ft (~87 m) (Fig. 5).

4.3.2. Succession type

The sedimentological analysis, and the ichnological assemblage of these repetitive successions allowed us to identify the common patterns between them. These can be divided into three parts (Fig. 7). The lower part begins with massive bioclastic mudrocks (Mb), bioclastic sandstones (Sb) or bioclastic conglomerates (Gb) and thicknesses between ~3 ft (~0,9 m) and ~10 ft (~3 m). These vary transitionally to massive (Mm) or horizontal lamination mudrocks (Mh) occasionally bioturbated by *Phycosiphon* (BI = 0–5) but with punctual record (Fig. 7). These mudrocks exhibit lenticular bedding (Htl) and the occurrence of *Teichichnus* (BI = 1–2). Moreover, syneresis cracks (Ms) and iron and siderite nodules are observed (Fig. 7). Thicknesses vary between ~20 ft (~6 m) and ~90 ft (~27 m). However, there is a typical succession where the thickness of this lithology is greater than the others ~200 ft (~61 m). At the middle part, the succession changes progressively to massive (Sm) and horizontal lamination silty sandstones (Sh) with thin and medium beds of bioturbated mudrocks by *Ophiomorpha*, *Taenidium*, *Thalassinoides*, and rarely *Teichichnus* (BI = 2–4). These facies exhibit massive structure (Sm), horizontal lamination (Sh), wavy bedding (Htw), as well as planar cross-bedding (Sp), and asymmetrical ripples (Sr) (Fig. 7). The thicknesses of this part of the succession vary between ~10 ft (~3 m) and ~25 ft (~8 m). Sometimes and less frequently, there is also some hummocky cross-stratification (HCS), convolute lamination (Sc), and symmetrical ripples (Sw; Fig. 7). Then, the succession passes upward to massive medium/fine sandstones (Sm), and sometimes coarse-grained, with organic matter fragments, and the ichnological assemblage of *Dactyloidites*, *Ophiomorpha*, *Skolithos*, and *Thalassinoides* (BI = 2–4) or with punctual record of *Macaronichnus* and/or *Ophiomorpha* (Fig. 7). Occasionally and with punctual record the ichnoassemblage consisting of *Conichnus*, *Cylindrichnus*, *Dactyloidites*, *Ophiomorpha*, *Skolithos* and *Thalassinoides* (BI = 2–5) is also observed. They present horizontal lamination (Sh), planar cross-bedding (Sp), trough cross-bedding (St), flaser (Htf) and wavy bedding (Htw), asymmetrical ripples (Sr) and, to a lesser extent, symmetrical ripples (Sw) (Fig. 7), and thicknesses between ~10 ft (~3 m) and ~25 ft (~8 m). At the upper part, the succession passes upward to medium/fine-grained bioturbated sandstones with massive structure (Sm), horizontal lamination (Sh), and low angle cross-bedding sandstones (Sa) (Fig. 7). Likewise, this upper part can be characterized by mudrocks with massive structure (Mm), horizontal lamination (Mh), and lenticular bedding (Htl) bioturbated by *Teichichnus* (BI = 1–2), as well as coal thin beds (Co), and massive (Sm) and horizontal lamination (Sh) fine-to coarse-grained sandstones sometimes with a punctual record of *Macaronichnus* and/or *Ophiomorpha* (BI = 2–4). These sandstones present variations to mudrocks and carbonaceous mudrocks with the presence of rhizoliths (Fig. 7). The upper part of the succession presents thicknesses between ~10 ft (~3 m) and ~20 ft (~6 m).

This repetitive coarsening upward succession type is interrupted by massive medium-to coarse-grained sandstones (Sm), massive conglomeratic sandstones (Sm) and/or massive polymictic granule-sized matrix-supported conglomerates (Gmm) with a high content of organic matter fragments, and erosive bases, as well as load casts (Slc), flame structures (Sf), and bioturbated by *Ophiomorpha* and *Taenidium* (BI = 1–2) (Fig. 7). Sometimes, normal gradation from granule-sized matrix-supported conglomerates (Gng), and conglomeratic sandstones to medium-, fine-grained sandstones occur (Fig. 7). At other times there is a bigradational trend: inverse gradation from fine/medium-grained sandstones (Sig) to conglomeratic sandstones and granule-sized matrix-supported conglomerates, and again normal gradation (Sng) to medium/coarse-grained sandstones. Occasionally, rhizoliths towards the top are observed. The most common thicknesses of these are between ~1 ft (~0,3 m) and ~10 ft (~3 m).

5. Interpretation and discussion

5.1. Depositional environment: fluvial-dominated deltaic system

The registered sedimentological features, as the frequent progradational trend (coarsening upward), the presence of sandstones and conglomerates (Sm, Gmm, Gcm) with erosive bases, the predominance of unidirectional structures such as asymmetric ripples (Sr), medium beds of sandstones with normal gradation (Sng, Gng) are associated with the development of channels (MacEachern et al., 2005; Coates and MacEachern, 2007). The previous facies association, together with the occurrence of coal beds (Co), the high content of organic debris, as well as the occurrence of massive sandstones (Sm) and massive mudrocks (Mm) with rhizoliths, together with the ichnological information, including composition, diversity and abundance of ichnoassemblages, allow the interpretation of a transitional system, more specifically a deltaic system (MacEachern et al., 2005; Bhattacharya, 2006). Furthermore, the dominance in time of these characteristics throughout the succession allows us to interpret a fluvial-dominated deltaic setting, characterized by variations in the coastline with continuous shallowing up sequences (Johnson and Dashtgard, 2014; Dalrymple et al., 2015; Dashtgard and La Croix, 2015; Ainsworth et al., 2017; Shchepetkina et al., 2019; Maselli et al., 2020) (Fig. 8).

The occurrence of some beds with flaser (Htf) and wavy bedding (Htw) and mud drapes associated, as well as hummocky cross-stratification (HCS) associated with interbedded sandy and muddy deposits, allows us to interpret local tidal influence on the system with sporadic storms (Dalrymple et al., 1990, 1992; Dashtgard et al., 2009; Desjardins et al., 2012; Shchepetkina et al., 2019). The punctual record of symmetrical ripples (Sw) could be associated with wave processes (Dalrymple et al., 1990, 1992; Bann et al., 2008). The presence of convolute lamination (Sc) at some intervals and occasional associated hummocky cross-stratification (HCS) and symmetrical ripples (Sw), also reflect sudden episodes of storms (Arnott and Southard, 1990; Frey, 1990; Bann et al., 2008). In this context, bioclastic deposits (Gb, Sb, Mb) could be related to rapid and short-time transgressive pulses (Savrda et al., 1993; Cattaneo and Steel, 2003; Buatois et al., 2012; Dí ez – Canseco et al., 2015; Schultz et al., 2020). After the short-time transgressive phase, the sedimentary environment usually returns to the previous conditions quickly. Conditions of a deeper/distal marine environment are not maintained over time but locally registered (e.g., 1833 ft–1811 ft; ~558.7 m–~552 m) (Fig. 5). However, at some intervals, the bioclastic deposits change progressively to laminated mudrocks (Mh) with few calcareous microfossils and low bioturbation, which could be related to a flooding phase in a confined interdistributary bay-type context and/or stagnant waters (Buatois et al., 2012; Dí ez – Canseco et al., 2015) (e.g., 1442 ft–1246 ft; ~439.5 m–~379.8 m; Fig. 5). In some intervals, medium beds of fine-to medium-grained sandstones with horizontal lamination (Sh) and low-angle cross-bedding (Sa), and bioturbation associated with *Macaronichnus*, and/or *Ophiomorpha* (BI = 3–4), typically occur twice at the top of the progradational

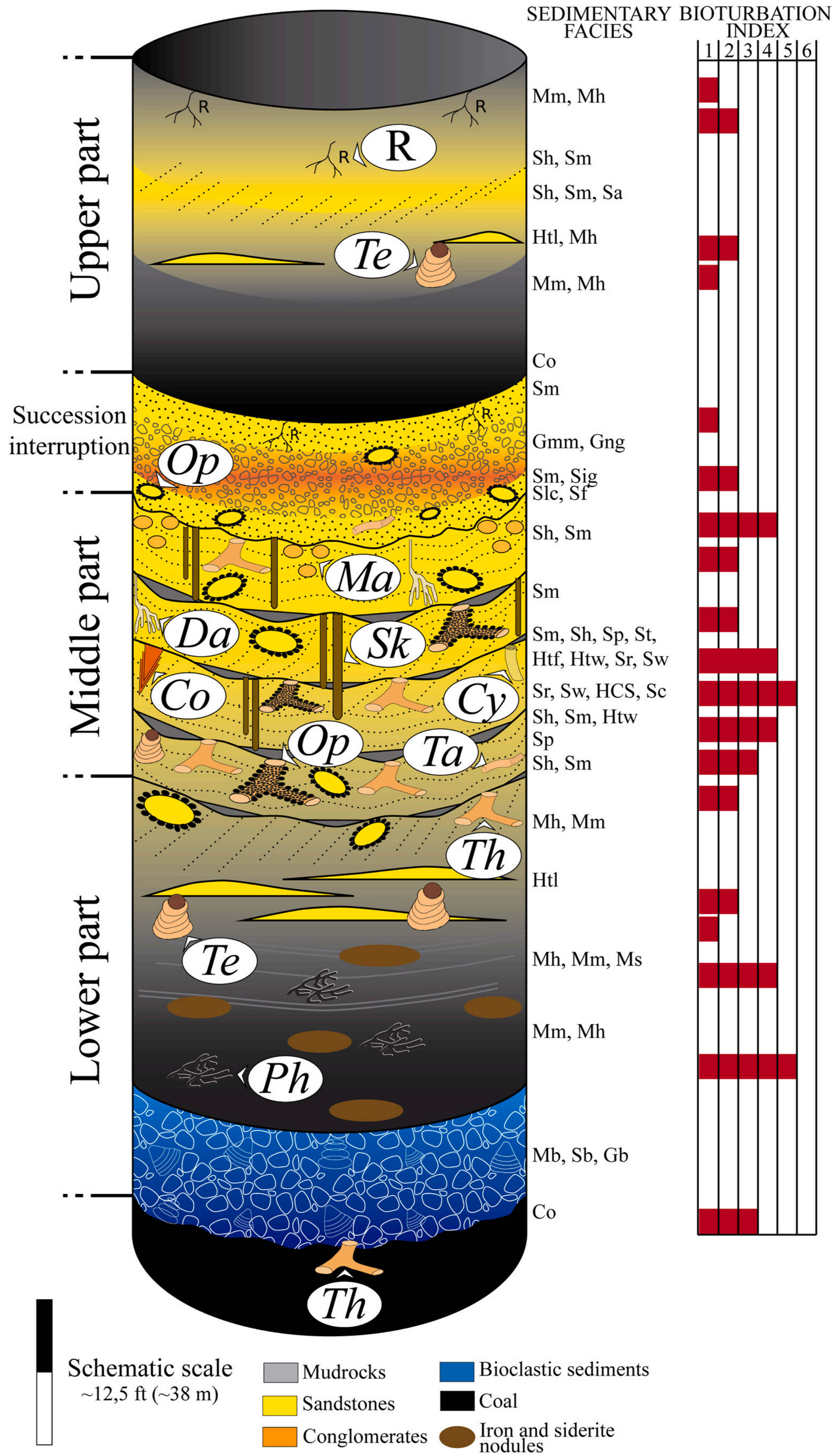

Fig. 7. Succession type found in the study succession with characteristic facies evolution and differentiated trace fossils. Note: *Conichnus* (*Co*), *Cylindrichnus* (*Cy*), *Dactyloidites* (*Da*), *Macaronichnus* (*Ma*), *Ophiomorpha* (*Op*), *Phycosiphon* (*Ph*), Rhizoliths (R), *Skolithos* (*Sk*), *Taenidium* (*Ta*), *Teichichnus* (*Te*), and *Thalassinoides* (*Th*). For facies codes see Table 1.

cycle, could be related to high-energy conditions on the beach-like environments (Pemberton et al., 2001; Buatois et al., 2012).

The interpreted generalized fluvial-dominated deltaic system, with the secondary, minor, tidal and wave influence, is supported by the ichnological record. The low abundant and moderate diverse trace fossil assemblage could be related to a stressful environment for macrobenthic trace maker communities (Buatois et al., 1997; MacEachern and Gingras, 2007), favouring the preservation of physical sedimentary structures (MacEachern et al., 2005; Buatois and Mángano, 2011). Some levels that register a higher abundance and diversity of traces (where *Conichnus*, *Cylindrichnus*, *Dactyloidites*, *Ophiomorpha*, *Skolithos*, *Teichichnus*, *Thalassinoides* can be recognized) (e.g., 1226 ft–1223 ft; ~373.7 m–~372.8 m) (Fig. 5) could be associated with mixed delta conditions where the fluvial domain decreases, and the tidal-wave influence increases (Bhattacharya and Giosan, 2003; Buatois et al., 2005; Bayet-Goll and Neto de Carvalho, 2020; Moyano Paz et al., 2020). However, these conditions do not last over time and are interrupted by the establishment of conditions with fluvial domain.

The presence of a high organic debris content, low bioturbation index (*Ophiomorpha* and/or *Taenidium*), together with deposits showing erosive bases and mainly normal gradations (Sng, Gng) with a thickness between ~0,5 ft and 3 ft, and bigradational trends, could be associated with the influence of multiple distributary channels providing hypopychnic feathers during normal fluvial discharges, and hyperpychnic during extraordinary river discharges (Mulder et al., 2003; MacEachern et al., 2005; Bhattacharya and MacEachern, 2009; Buatois et al., 2011, 2019; Zavala et al., 2011; Dí ez – Canseco et al., 2015; Zavala and Pan, 2018). In this context, an increase in the input of fresh water into the environment is envisaged, determining a considerable decrease in salinity, and then significant variations in a brackish setting (Buatois et al., 2005). This fact, together with the increase in both turbidity and sedimentation rate, would have negatively affected the development of benthic communities (Gingras et al., 1998; MacEachern et al., 2005), evidencing the dominant incidence of fluvial processes in the ecological and depositional environment, and the secondary, minor, tidal and wave influence (Bhattacharya and Giosan, 2003; Buatois et al., 2005; Bayet-Goll and Neto de Carvalho, 2020; Moyano Paz et al., 2020). The punctual record of massive oligomictic clast-supported conglomerates (Goc) show transport and deposition of sediments in these high-energy environments, but some of the clasts originated from within the basin of deposition and were eroded from penecontemporaneous sediments (Collinson and Mountney, 2019).

5.2. Sub-environments into the fluvial-dominated deltaic system

In this generalized deltaic system with fluvial domain interpreted for the study interval, facies association and ichnological analysis allow recognition of different sub-environments, as prodelta-bay, distal delta front, proximal delta front (subaqueous distributary channels, distributary mouth bars), lower delta plain-interdistributary bays, lower delta plain-floodplain, swamps, beach-like, lower delta plain-crevasse splays, channel, bars (Fig. 8). These different sub-environments are replaced several times through the studied interval (Fig. 8).

5.2.1. Facies association 1 - prodelta - bay (FA1)

Description. Characterized by massive mudrocks (Mm), and horizontal lamination mudrocks (Mh), with the exclusive presence of *Phycosiphon* in the first centimeters after the occurrence of bioclastic sediments (Mb, Sb, Gb), together with a moderate to low occurrence of marine calcareous microfossils (Project Contrato RC 494, 2017). The

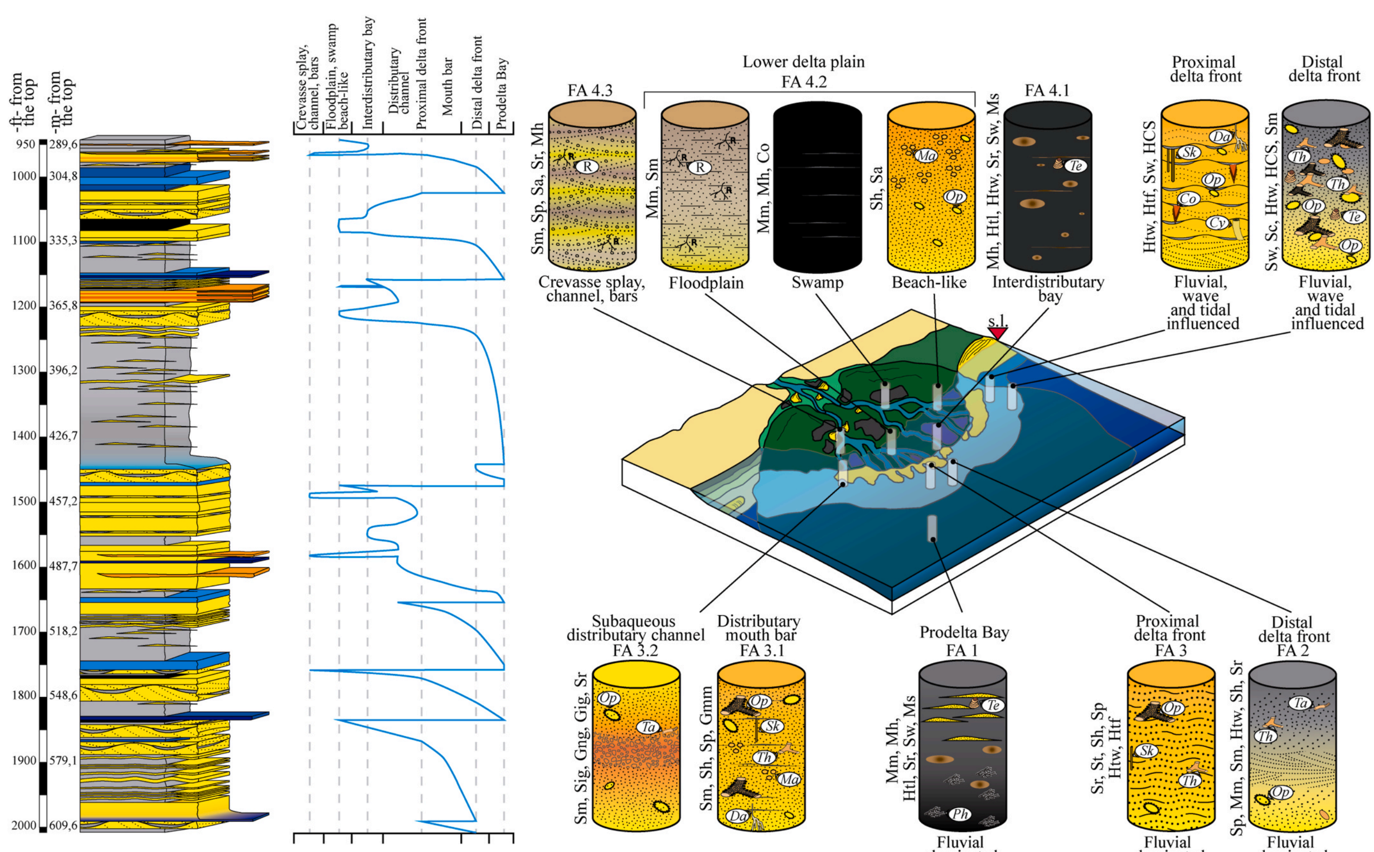

Fig. 8. Summarizing sketch showing the differentiated sub-environments of a fluvial-dominated deltaic system interpreted for the studied succession. Note: *Conichnus* (*Co*), *Cylindrichnus* (*Cy*), *Dactyloidites* (*Da*), *Macaronichnus* (*Ma*), *Ophiomorpha* (*Op*), *Phycosiphon* (*Ph*), Rhizoliths (R), *Skolithos* (*Sk*), *Taenidium* (*Ta*), *Teichichnus* (*Te*), and *Thalassinoides* (*Th*). FA facies association. S.l sea level. For facies codes see Table 1.

bioturbation indexes are 0 and when the specific occurrence of *Phycosiphon* occurs it is between 4 and 5. At the top of these facies, there is the occurrence of a) lenticular bedding (Htl) occasionally with *Teichichnus* (BI = 1–2), asymmetrical and symmetrical ripples (Sr, Sw), syneresis cracks (Ms), and siderite nodules and/or b) massive sandstones (Sm) with erosional base truncating the succession.

Interpretation. Bioclastic sediments could represent singles episodes of transgressive lags (Gingras et al., 1999, 2012a; MacEachern et al., 1999; Cattaneo and Steel, 2003). The subsequent conditions with the unique occurrence of calcareous marine microfossils throughout the succession, domain of mudrocks, and the presence of *Phycosiphon*, could be associated with the punctual record of sediments deposited under the most marine conditions of the system related to prodelta environments (Fig. 8). Low bioturbation index and low diversity in this scenario, represent the influence of the fluvial system (MacEachern et al., 2005; Buatois et al., 2012). The occurrence of *Phycosiphon* also could be linked to the opportunistic character of the producer organism in an environment with food availability (Wetzel, 2010; Rodrí guez – Tovar et al., 2014; Celis et al., 2018), which would be related to high inputs of organic matter from the fluvial system. Towards the top, the facies association described in a) could represent quiet hydrodynamic situations in bay conditions because the conditions of the prodelta are not maintained over time due to the fact that the flood is not representative (Bhattacharya, 2006). There is an overall shallowing-upward facies succession, associated with a trend from more marine to more nonmarine facies, but commonly without the deposition of thick sands (Bhattacharya, 2006) represented by the local occurrence of lenticular bedding (Htl), and symmetrical ripples (Sw) in this case, that would show the tidal and wave influence. However, the dominance of the fluvial system is represented by the continuous occurrence of asymmetrical ripples (Sw) associated with unidirectional currents, and the low bioturbation indexes associated with stressful conditions. Moreover, syneresis cracks (Ms), and siderite nodules reveal salinity fluctuations in the system (MacEachern et al., 2005; Buatois et al., 2012; Gingras et al., 2012a; Dí ez – Canseco et al., 2015). The sequence is sometimes interrupted by the succession described in b) related to distributary channels (Bhattacharya, 2006). The overall shallowing-upward facies succession from massive or laminated mudrocks (Mm, Mh) with *Phycosiphon* to lenticular bedding (Htl) with *Teichichnus* represents the transition from prodelta to bay environments (Bhattacharya and Walker, 1991; Bhattacharya, 2006).

5.2.2. Facies association 2 - distal delta front (FA2)

Description. Characterized by mudrocks, muddy sandstones, and fine-grained sandstones with planar cross-bedding (Sp), massive structure (Mm, Sm), wavy bedding (Htw), horizontal lamination (Sh), asymmetrical ripples (Sr), moderate bioturbation indexes (2–4), and the record of *Ophiomorpha*, *Taenidium*, and *Thalassinoides*. Occasionally there are the occurrence of an association of facies characterized by symmetrical ripples (Sw), convolute lamination (Sc), and hummocky cross-stratification (HCS).

Interpretation. The fine-grain size sediment domain, muddy sandstones with planar cross-bedding (Sp), and the absence of dwelling structures of suspension feeding organisms, suggests distal environments within the deltaic system (MacEachern et al., 2005; Gingras et al., 2011; Buatois et al., 2012; Moyano Paz et al., 2020). However, the variable concentration of organic matter, together with the low ichnodiversity, shows the fluvial domain on the succession (Buatois et al., 2005; MacEachern et al., 2005; Bhattacharya, 2006) (Fig. 8). This succession is overlying the characteristic facies of the prodelta-bay or transgressive lag deposits, and towards the top, it transitionally changes to coarser sandstones from the proximal deltaic front (Fig. 8). The facies association described could correspond with the record of the influence of waves and storms (Arnott and Southard, 1990; Frey, 1990; MacEachern et al., 2005; Coates and MacEachern, 2007; Bann et al., 2008; Buatois et al., 2012; Solórzano et al., 2017; Moyano Paz et al., 2020).

5.2.3. Facies association 3 - proximal delta front (FA3)

Description. It is characterized by well-selected fine-to medium grained sandstones, with asymmetrical ripples (Sr), trough cross-bedding (St), horizontal lamination (Sh), wavy (Htw) and flaser bedding (Htf), diffuse planar cross-bedding (Sp), and organic debris, as well as bioturbation indexes between 2 and 3, and the occurrence of the assemblage or exclusive ichnogenus such as *Ophiomorpha*, *Skolithos* and/or *Thalassinoides*. The occurrence of wavy (Htw), flaser bedding (Htf), and from paired mud drapes within cross-beds, sometimes with *Ophiomorpha*, occurs as punctual record, as well as the occurrence of symmetrical ripples (Sw), and hummocky cross-stratification (HCS).

Interpretation. According to the sedimentological and ichnological characteristics raised in the distal delta front and those evidenced in this facies association, a prograding trend can be interpreted. The most proximal conditions are reflected in the low indexes of bioturbation together with the dominance of sandy sediments with sedimentary structures of unidirectional currents that reveal an environment with high-energy conditions, and well oxygenated waters associated with river discharge (Gingras et al., 1998; Moslow and Pemberton, 1988; MacEachern et al., 2005; Coates and MacEachern, 2007; Buatois and Mángano, 2011; Solórzano et al., 2017; Moyano Paz et al., 2020) (Fig. 8). The interbedded of bioturbated sandstones and mudrocks (Htw, Htf), and mud drapes supports the interpretation of tidal influence (Dalrymple and Choi, 2007; Buatois et al., 2012; Dí ez – Canseco et al., 2015). The occurrence of symmetrical ripples (Sw), and hummocky cross-stratification (HCS) reveals the local influence of waves and/or storms (Arnott and Southard, 1990; Frey, 1990; Coates and MacEachern, 2007; Bann et al., 2008). This association of facies is sometimes interrupted by distributary mouth bar and, subaqueous distributary channels deposits.

5.2.3.1. Facies association 3.1 - distributary mouth bars. **Description.** It consists of medium-to fine-grained sandstones with massive structure (Sm), horizontal lamination (Sh), and planar cross-bedding (Sp). Coarsening-upward trends from the sandstones to granule-sized matrix-supported conglomerate (Gmm) is recorded. The bioturbation index varies between 2 and 4, and it is characterized by the ichnological association or by the exclusive occurrence of *Dactyloidites*, *Macaronichnus*, *Ophiomorpha*, *Skolithos* and/or *Thalassinoides*.

Interpretation. The sedimentary structures identified are typical of high energy environments with sheet flows, and migration of two-dimensional dunes where the underlying succession presents the sedimentological and ichnological characteristics of the subaqueous distributary channels (Buatois et al., 2005, 2012, 2012; MacEachern et al., 2005; Coates and MacEachern, 2007) (Fig. 8). The coarsening-upward trend indicates continuous progradational succession.

5.2.3.2. Facies association 3.2 - subaqueous distributary channels. **Description.** It is represented by massive medium-to coarse-grained sandstones (Sm) with variations to conglomeratic sandstones (Sig), and granule-sized matrix-supported conglomerates with normal and inverse gradation (Gng, Gig) -bigradational trend, asymmetrical ripples (Sr), as well as erosive bases, organic matter debris and bioturbation indexes between 0 and 2 with the exclusive presence of *Ophiomorpha* or *Taenidium*. *Ophiomorpha* present smaller sizes (~0.5–1 cm in diameter, and 3–4 cm long). Furthermore, some associated flame structures (Sf), and load casts (Slc) are recognized. The punctual flaser bedding (Htf), and interbedded mud-drapes record are also given.

Interpretation. These lithological and ichnological characteristics suggest deposition in a brackish to marine environment, with episodic sedimentation of currents with high-water-turbidity in a fluvial-dominated delta front environment, probably associated with collapses of the channel bar deposits, or high-density hyperpychnic flows (Mulder and Syvitski, 1995; Bhattacharya, 2006; Buatois et al., 2011; Zavala and Pan, 2018; Moyano Paz et al., 2020) (Fig. 8). The absence of dwelling structures of suspension-feeders, together with the low diversity, is characteristic. Stressful environmental conditions limit the development of a stable, diverse and abundant macrobenthic community, determining low indexes of bioturbation (BI = 0–2) generated mainly by deposit-feeders organisms (Gingras et al., 1998; Moslow and Pemberton, 1988; MacEachern et al., 2005; Coates and MacEachern, 2007; Buatois and Mángano, 2011). The small sizes exhibited by *Ophiomorpha* may indicate fluctuations in salinity conditions (MacEachern et al., 2005; Coates and MacEachern, 2007; Gingras et al., 2011). The sporadic record of flaser bedding (Htf), as well as the occasional occurrence of interbedded mud-drapes, reveals the local tidal influence on the system (Dalrymple and Choi, 2007).

5.2.4. Facies association 4 - lower delta plain

5.2.4.1. Facies association 4.1 - lower delta plain: interdistributary bays with tidal and wave influence (FA4.1). **Description.** It is characterized by massive mudrocks (Mm), horizontal lamination mudrocks (Mh), and lenticular bedding (Htl), with occasional bivalves and gastropods fragments, and undifferentiated shells, and to a lesser extent wavy bedding (Htw), as well as asymmetrical ripples (Sr), symmetrical ripples (Sw), syneresis cracks (Ms), and siderite nodules. Bioturbation indexes are very low (BI = 0–2) and only the ichnogenus *Teichichnus* can be recognized. Calcareous microfossils are near absent, except for a few benthic foraminifera (Project Contrato RC 494, 2017).

Interpretation. Syneresis cracks (Ms), and siderite nodules reveal salinity fluctuations in the system (MacEachern et al., 2005; Buatois et al., 2012; Gingras et al., 2012a; Dí ez – Canseco et al., 2015). These ichnological and lithological features can be associated with deposits of muddy and mixed plains, accumulated in interdistributary bays that take place after transgression episodes (transgressive lags) and under quiet conditions and low turbidity, but with a high content of organic matter (Gingras et al., 1999, 2012a; MacEachern et al., 1999; Cattaneo and Steel, 2003; Buatois et al., 2012) (Fig. 8). The influence of unidirectional currents is evidenced in Sr. The tidal influence in these systems is associated with lenticular bedding (Htl) and mudrocks dominance (Buatois et al., 2012; Gingras et al., 2012; Dí ez – Canseco et al., 2015), and the wave influence may be associated with the symmetrical ripples (Buatois et al., 2012).

5.2.4.2. Facies association 4.2 - lower delta plain: floodplain, swamp, beach-like (FA4.2). **Description.** The previous facies association, linked to interdistributary bays, together with the occurrence of very fine- and fine-grained horizontal lamination sandstones (Sh), massive sandstones (Sm) with rhizoliths, massive mudstones (Mm), massive carbonaceous mudrocks (Mm), horizontal lamination mudrocks (Mh), and coal beds (Co), represent this sub-environment. In some rare cases, thin and medium beds of fine-medium-grained sandstones with low angle cross-bedding (Sa) and horizontal lamination (Sh) with intense bioturbation (BI = 4–5) associated with *Macaronichnus* and/or *Ophiomorpha* typically occur at the top of the progradational cycle.

Interpretation. Variations from fine-grained sediments (Mm, Mh) to coal beds (Co) particularly indicate the development of peat bogs in swampy areas constantly waterlogged, enabling the accumulation and preservation of organic matter (Retallack, 2001; Buatois et al., 2012) (Fig. 8). However, in this same environment and far from these swampy areas, the occurrence of fine-grained deposits with root traces fossils indicates low energy traction currents developed in the subaerial delta plain (MacEachern et al., 2005, 2007b, 2007b; Bhattacharya, 2006; Buatois et al., 2012). Fine-grained sandstones and mudrocks are interpreted to represent thin sheet sands and distal portions of splays deposited during river flood conditions (Heldreich et al., 2017). The record of Sh and Sa with the trace fossils *Macaronichnus* and/or *Ophiomorpha*, even if it is very scarce, could reveal beach-like environments (Pemberton et al., 2001; Buatois et al., 2012).

5.2.4.3. Facies association 4.3 - lower delta plain: crevasse splays, channel, bars (FA4.3). **Description.** It is associated with the described facies of the lower delta plain; there are also fine-to coarse-grained massive sandstones (Sm), planar cross-bedding (Sp), low-angle cross-bedding (Sa), asymmetrical ripples (Sr), and to a lesser extent, some thin horizontal lamination mudrocks beds (Mh). Settings with root trace fossils are also present.

Interpretation. High and low-angle cross-bedding is common in sandy crevasse-splay deposits, but there is also evidence for the cessation of current discharge, in the form of mudrock and sandstones beds with rhizoliths (Bridge, 2006). Overbank crevasse splay deposits closest to the main channel can be confused with upper channel-bar deposits displaying a progressive decrease in grain size with increasing distance from the channel margin (Bridge, 2006; Heldreich et al., 2017). The current structures generated in the sandstones (Sr) could show the influence of channels in this area (Dalrymple and Choi, 2007; Johnson and Dashtgard, 2014; Dalrymple et al., 2015; Dashtgard and La Croix, 2015). The Sa facies could register the down current migration of point and longitudinal bars deposited by traction from relatively weak currents that approach upper-flow regime conditions for the size of sediment being deposited (Picard and High, 1973). This makes it difficult to interpret this sub-environment, so we consider that it represents a crevasse splay adjacent to fluvial and distributary channel bodies.

5.3. Wave and tidal influenced: the ichnological record

Bioclastic-rich sediments (Gb, Sb, Mb) with approximate thicknesses between ~3 ft (~0,9 m) and ~10 ft (~3 m), associated with transgressive pulses, on some occasions change progressively to muddy and fine sandy sediments with horizontal lamination (Sh), symmetrical ripples (Sw), and locally hummocky cross-stratification (HCS). Its particular characteristic is a higher ichnodiversity (*Ophiomorpha*, *Teichichnus*, *Thalassinoides*) and abundance of trace fossils (BI = 3–5) than are observed in other intervals. Then a coarsening-upward to medium-fine sandstones, flaser bedding (Htf) with mud drapes is registered, showing an ichnoassemblage consisting of *Conichnus*, *Cylindrichnus*, *Dactyloidites*, *Ophiomorpha*, *Skolithos* and *Thalassinoides*. In particular, the intervals that present these characteristics are few and these conditions do not last over time, being rapidly interrupted by a) medium-to fine-grained sandstones with horizontal lamination (Sh), and planar cross-bedding (Sp), and BI = 2–4 with the ichnological association or the exclusive occurrence of *Macaronichnus*, *Ophiomorpha*, and/or *Skolithos*, characteristics of the mouth bar; and/or b) medium to fine sandstones with normal and inverse gradation (Sng, Sig), as well as erosive bases, organic matter debris and bioturbation indexes between 0 and 2 with the exclusive presence of *Ophiomorpha* or *Taenidium* characteristics of the distributary channels. Thus, the dominant ichnological and lithological features contrast with those previously described.

These punctual records can probably be associated with episodes where fluvial control decreases, allowing the development of a delta front under mixed conditions (Bhattacharya and Giosan, 2003; MacEachern et al., 2005; Bhattacharya, 2006; Coates and MacEachern, 2007; Bann et al., 2008; Buatois et al., 2012; Bayet-Goll and Neto de Carvalho, 2020; Canale et al., 2020; Moyano Paz et al., 2020) (Fig. 8). The association of facies interpreted as beach-like conditions is not related to this mixed environment, since the previous facies to these deposits are associated with the distributary channel and the later facies with the lower delta plain. Therefore, beach-like environments are not directly considered a deposit associated with wave processes.

The associated environmental conditions favour the establishment of a more diverse and abundant macrobenthic trace maker community as reflected in the ichnological record. However, the next progradation of the deltaic system through the mouth bar/distributary channels, prevents maintenance of these conditions.

The contact surfaces separating these two scenarios (deltaic systems fluvial-dominated vs mixed) could represent regressive surfaces

(MacEachern et al., 2007b; Moyano Paz et al., 2020), but a more detailed analysis is needed before any conclusive interpretation.

Similar examples have been recognized in tropical deltas (Buatois et al., 2012). Sequences that vary along the coastline but also vertically have been identified and characterized as fluvial deltas dominated with tidal and wave influence. Even, storm dominated successions interrupting the river sequence has been identified (Buatois et al., 2012). In this alternation of conditions, each one of them persists over time and these variations are observed along the coastline, which gives rise to the establishment of ecological niches and stable palaeoenvironmental conditions at each stage. In our case study, low abundance and moderate diversity of trace fossils, as well as unidirectional structures, and erosive bases predominate throughout the entire succession and therefore, in general terms the fluvial domain has been interpreted.

5.4. Prospective considerations

The deposits associated with the fluvial-marine transition zone are of particular interest as hydrocarbon reservoirs (Whateley and Pickering, 1989; Shields and Strobl, 2010). However, depending on the position within this zone, fluvial, tidal and/or wave conditions may dominate, which determines variations in the facies association (Dalrymple and Choi, 2007; Howell et al., 2008). In this sense, the internal architecture and the heterogeneity of the facies, not only lateral but also vertical, are primary factors of great importance in the quality of the reservoir (Miall, 1988; Slatt, 2006).

Our detailed analysis suggests that the studied succession drilled by the ANH-SSJ-Nueva Esperanza-1X stratigraphic well, was deposited in a fluvio-dominated delta setting during part of the Oligocene. Obtained data are in agreement with the general deltaic environment previously interpreted for the Ciénaga de Oro Formation (Duque-Caro, 1972; Dueñas, 1983; Guzmán, 2007; Bermúdez et al., 2009; Mora et al., 2017, 2018; Osorio-Granada et al., 2020; Manco– Garc é s et al., 2020). However, due to the study succession obeys a highly dynamic depositional context where lateral and vertical variations of facies are evident and frequent, it is necessary to conduct high-resolution sedimentological and ichnological studies to evaluate the continuity, and therefore, the prospectivity of the successions with the same chronostratigraphic range because not all the interpreted sub-environments represent ideal conditions as reservoirs.

6. Conclusions

Sedimentological and ichnological analysis of a core drilled in the Oligocene deposits of the Sinú-San Jacinto Basin (SSJB) (Colombian Caribbean) allows interpret the development of a fluvial-dominated delta. The studied interval corresponds to a siliciclastic succession with approximately 1069 ft (~326 m) thick. The sedimentological analysis allows the differentiation of dominant facies, with predominant lithologies such as conglomerates, sandstones, mudrocks, bioclastic sediments, as well as coal beds. Ichnological analysis reveals a low abundant, and moderately diverse trace fossil assemblage, consisting of ten ichnogenera *Conichnus*, *Cylindrichnus*, *Dactyloidites*, *Macaronichnus*, *Ophiomorpha*, *Phycosiphon*, *Skolithos*, *Taenidium*, *Teichichnus*, and *Thalassinoides*, together with rhizoliths. The interval studied presents multiple coarsening upward metric successions with a regular order of facies and ichnological assemblage that allows establishing a succession type.

Integration of sedimentological and ichnological information allows us to interpret the complexity of the fluvial-dominated deltaic system as reflected in its evolution over time, and in the different sub-environments characterized: prodelta bay, distal delta front, proximal delta front, mouth bars, distributary channels, and lower delta plain. Thus, even the fluvial processes were dominant in the deltaic system; this was affected by the tidal and wave influence. Throughout the succession, the fluvial-dominated deltaic system was punctuated by the episodic development of a mixed deltaic system.

The detailed ichnological analysis conducted shows the usefulness of ichnology for the characterization of complex environments, such as deltaic ones, given the response of tracemakers to stressful and highly variable conditions in these environments. This reveals special interest due to the economic importance of the studied area.

Authorship statement

Celis, S.A: Conceptualization, Methology, Writing - Original Draft, Formal analysis. Rodríguez-Tovar, F.J: Conceptualization, Methology, Writing - Review & Editing, Supervision.Giraldo-Villegas, C: Writing - Review & Editing, Visualization. Pardo-Trujillo, A: Writing - Review & Editing

Declaration of competing interest

The authors declare that they have no known competing financial interests or personal relationships that could have appeared to influence the work reported in this paper.

Acknowledgements

We would like to thank Dr. Pazos (JSAES Guest Editor) and two anonymous reviewers by constructive comments and suggestions. Thanks to the National Hydrocarbons Agency-ANH, and *Ministerio de Ciencia, Tecnología e Innovación - Minciencias* to allow the study of well-core (project Contrato RC 494–2017). The Vicerrectoría de Investigaciones y Posgrados and the Instituto de Investigaciones en Estratigrafía-IIES of Universidad de Caldas gave economic and logistic support. The research was conducted within the "Ichnology and Palaeoenvironment RG" (UGR). Financial support of Rodríguez-Tovar was provided by scientific Projects CGL 2015-66835-P and CTM 2016-75129-C3-2-R (Secretaría de Estado de I + D + I, Spain), and B-RNM-072-UGR18 (FEDER Andalucía), and Research Group RNM-178 (Junta de Andalucía). Funding for open access charge: Universidad de Granada / CBUA. Thanks to Fabian Gallego for his contribution in some sedimentological discussions.

References

Abad, M., Ruiz, F., Pendón, J.G., Tosquella, J., González–Regalado, M.L., 2006. Escape and equilibrium trace fossils in association with *Conichnus conicus* as indicators of variable sedimentation rates in Tortonian littoral environments of SW Spain. Geobios 39, 1–11.

Agirrezabala, L.M., de Gibert, J.M., 2004. Paleodepth and paleoenvironment of *Dactyloidites ottoi* (Geinitz, 1849) from lower cretaceous deltaic deposits (Basque–Cantabrian basin, west Pyrenees). Palaios 19, 276–291.

Ainsworth, R.B., Flint, S.S., Howell, J.A., 2008. Predicting coastal depositional style: influence of basin morphology and accommodation to sediment supply ratio within a sequence stratigraphic framework. In: Hampson, G.J., Steel, R.J., Burgess, P.M., Dalrymple, R.W. (Eds.), Recent Advances in Models of Shallow-Marine Stratigraphy, vol. 90. SEPM Special Publication, Tulsa, Oklahoma, pp. 237–263.

Ainsworth, R.B., Vakarelov, B.K., Nanson, R.A., 2011. Dynamic spatial and temporal prediction of changes in depositional processes on clastic shorelines: toward improved subsurface uncertainty reduction and management. APPG Bullet. 95, 267–297.

Ainsworth, R.B., Vakarelov, B.K., MacEachern, J.A., Rarity, F., Lane, T.I., Nanson, R.A., 2017. Anatomy of a shoreline regression: implications for the high–resolution stratigraphic architecture of deltas. J. Sediment. Res. 87, 425–459.

Alfaro, E., Holz, M., 2014. Review of the chronostratigraphic charts in the Sinú–San Jacinto basin based on new seismic stratigraphic interpretations. J. S. Am. Earth Sci. 56, 139–169.

Alpert, S.P., 1974. Systematic review of the genus *Skolithos*. J. Paleontol. 48, 661–669.

Arnott, R.W., Southard, J.B., 1990. Exploratory flow–duct experiments on combined–flow bed configurations, and some implications for interpreting storm event stratification. J. Sediment. Petrol. 60, 211–219.

Astin, T.R., Rogers, D.A., 1991. 'Subaqueous shrinkage cracks' in the Devonian of Scotland reinterpreted. J. Sediment. Petrol. 61, 850–859.

Bann, K.L., Tye, S.C., MacEachern, J.A., Fielding, C.R., Jones, B.G., 2008. Ichnological and sedimentologic signatures of mixed wave– and storm–dominated deltaic deposits: examples from the Early Permian Sidney Basin, Australia. In: Hampson, G. J., Steel, R.J., Burgess, P.B., Dalrymple, R.W. (Eds.), Recent Advances in Models of Siliciclastic Shallow–Marine Stratigraphy, vol. 90. Society for Sedimentary Geology, Special Publication, pp. 292–332.

Baucon, A., Ronchi, A., Felletti, F., Neto de Carvalho, 2014. Evolution of crustaceans at the edge of the end–Permian crisis: ichnonetwork analysis of the fluvial succession of Nurra (Permian–Triassic, Sardinia, Italy). Palaeogeogr. Palaeoclimatol. Palaeoecol. 410, 74–103.
Bayet–Goll, A., Neto de Carvalho, C., 2020. Architectural evolution of a mixed-infuenced deltaic succession: lower-to-middle ordovician armorican quartzite in the southwest central Iberian zone, Penha Garcia formation (Portugal). Int. J. Earth Sci. 109, 2495–2526.
Belaústegui, Z., de Gibert, J.M., 2013. Bow-shaped, concentrically laminated polychaete burrows: a *Cylindrichnus concentricus* ichnofabric from the Miocene of Tarragona, NE Spain. Palaeogeogr. Palaeoclimatol. Palaeoecol. 381–382, 119–127.
Bermúdez, H.D., Alvarán, M., Grajales, J.A., Restrepo, L., Rosero, J.S., Guzmán, C., Ruiz, E., Navarrete, R., Jaramillo, C., Osorno, F., 2009. Estratigrafía y evolución geológica de la secuencia sedimentaria del Cinturón Plegado de San Jacinto. XII Congreso Colombiano de Geología. Paipa, Colombia, pp. 1–28.
Bermúdez, H.D., 2016. Esquema estratigráfico de secuencias del registro sedimentario del Cinturón Plegado de San Jacinto, Caribe colombiano. In: Extended abstract presented at the XII Simposio Bolivariano Exploración Petrolera en Cuencas Subandinas, September 26–28, Bogotá.
Bernal–Olaya, R., Mann, P., Escalona, A., 2015. Cenozoic tectonostratigraphic evolution of the lower Magdalena basin, Colombia: an example of an under– to overfilled forearc basin. In: Batolini, C., Mann, P. (Eds.), Petroleum Geology and Potential of the Colombian Caribbean Margin, vol. 108, pp. 345–398.
Bhattacharya, J.P., Walker, R.G., 1991. Facies and facies successions in river- and wave-dominated depositional systems of the Upper Cretaceous Dunvegan Formation, northwestern Alberta. Bull. Can. Petrol. Geol. 39, 165–191.
Bhattacharya, J.P., Walker, R.G., 1992. Deltas. In: Walker, R.G., James, N.O. (Eds.), Facies Models: Response to Sea-Level Change. Geological Association of Canada, St Johns, pp. 157–177.
Bhattacharya, J.P., Giosan, L., 2003. Wave-influenced deltas: geomorphological implications for facies reconstruction. Sedimentology 50, 187–210.
Bhattacharya, J.P., 2006. Deltas. In: Posamentier, H.W., Walker, R.G. (Eds.), Facies Models Revisited, vol. 84. Society of Economic Paleontologists and Mineralogists Special Publication, pp. 237–292.
Bhattacharya, J.P., MacEachern, J.A., 2009. Hyperpycnal rivers and prodeltaic shelves in the Cretaceous seaway of North America. J. Sediment. Res. 79, 184–209.
Boyd, R., Dalrymple, R., Zaitlin, B.A., 1992. Classification of clastic coastal depositional environments. Sediment. Geol. 80, 139–150.
Boyd, C., McIlroy, D., 2016. Three–dimensional morphology and palaeobiology of the trace fossil *Dactyloidites jordii* nov. isp. from the Carboniferous of England. Geobios 49, 257–264.
Bridge, J.S., 2006. Fluvial facies models: recent developments. In: Posamentier, H.W., Walker, R.G. (Eds.), Facies Models Revisited, vol. 84. SEPM (Society for Sedimentary Geology), Special Publications, pp. 85–170.
Bromley, R.G., 1990. Trace Fossils; Biology and Taphonomy, vol. 3. Unwin Hyman, London, p. 280. Special Topics in Paleontology.
Bromley, R.G., Milàn, J., Uchman, A., Hansen, K.S., 2009. Rheotactic *Macaronichnus*, and human and cattle trackways in Holocene beachrock, Greece: reconstruction of paleoshoreline orientation. Ichnos 16, 103–117.
Buatois, L.A., Mángano, M.G., Maples, C.G., Lanier, W.P., 1997. The paradox of nonmarine ichnofaunas in tidal rhythmites: integrating sedimentologic and ichnologic data from the Late Carboniferous of Eastern Kansas. Palaios 12, 467–481.
Buatois, L.A., Gingras, M.K., MacEachern, J.A., Mángano, M.G., Zonneveld, J.P., Pemberton, S.G., Netto, R.G., Martin, A.J., 2005. Colonization of Brackish–water systems through time, Evidence from the trace–fossil record. Palaios 20, 321–347.
Buatois, L.A., Mángano, M.G., 2011. Ichnology: Organism–Substrate Interactions in Space and Time. Cambridge University Press, p. 358.
Buatois, L.A., Saccavino, L.L., Zavala, C., 2011. Ichnologic signatures of hyperpycnal flow deposits in Cretaceous river–dominated deltas, Austral Basin, southern Argentina. In: Slatt, R.M., Zavala, C. (Eds.), Sediment Transfer from Shelf to Deep Water—Revisiting the Delivery System, vol. 61. AAPG Studies in Geology, pp. 153–170.
Buatois, L.A., Santiago, N., Herrera, M., Plink–Björklund, P., Steel, R.J., Espin, M., Parra, K., 2012. Sedimentological and ichnological signatures of changes in wave, river and tidal influence along a Neogene tropical deltaic shoreline. Sedimentology 59, 1568–1612.
Buatois, L.A., Mángano, M.G., Pattison, S.A.J., 2019. Ichnology of prodeltaic hyperpycnite-turbidite channel complexes and lobes from the upper cretaceous Praire Canyon member of the Mancos Shale, Book Cliffs, Utah, USA. Sedimentology 66 (5), 1825–1860.
Canale, N., Ponce, J.J., Carmona, N.B., Parada, M.N., Drittanti, D.I., 2020. Sedimentología e icnología de un delta fluvio-dominado, Formación Lajas (Jurásico Medio), cuenca Neuquina, Argentina. Andean Geol. 47, 179–206.
Cardona, A., Montes, C., Ayala, C., Bustamante, C., Hoyos, N., Montenegro, O., Ojeda, C., 2012. Tectonophysics from arc–continent collision to continuous convergence, clues from Paleogene conglomerates along the southern Caribbean–South America plate boundary. Tectonophysics 580, 58–87.
Cattaneo, A., Steel, R.J., 2003. Transgressive deposits: a review of their variability. Earth Sci. Rev. 62 (3–4), 187–228.
Cediel, F., Shaw, R.P., Cáceres, C., 2003. Tectonic assembly of the northern andean block. AAPG Memoir 79, 815–848.
Celis, S.A., Rodríguez–Tovar, F.J., Pardo–Trujillo, A., 2018. The *Phycosiphon* record in the ladrilleros–Juanchaco section (Miocene, Colombian Pacific): palaeoecological implications. Spanish J. Palaeontol. 33 (2), 277–288.
Clifton, H.E., Thompson, J.K., 1978. *Macaronichnus segregatis*: a feeding structure of shallow marine polychaetes. J. Sediment. Petrol. 48, 1293–1302.
Coates, L., MacEachern, J.A., 2007. The ichnological signatures of river- and wave-dominated delta complexes: differentiating deltaic and non-deltaic shallow marine successions, Lower Cretaceous Viking Formation and Upper Cretaceous Dunvegan Formation, West-Central Alberta. In: MacEachern, J.A., Bann, K.L., Gingras, M.K., Pemberton, S.G. (Eds.), *Applied Ichnology*. Society for Sedimentary Geology, Short Course Notes, vol. 52, pp. 227–255.
Collins, S.D., Johnson, H.D., Baldwin, C.T., 2019. Architecture and preservation in the fluvial to marine transition zone of a mixed–process humid–tropical delta: middle Miocene Lambir Formation, Baram Delta Province, north–west Borneo. Sedimentology 67, 1–46.
Collinson, J., Mountney, N., Thompson, D., 2006. Sedimentary Structures, third ed. Terra publishing, p. 302p.
Collinson, J., Mountney, N., 2019. Sedimentary Structures –, fourth ed. Dunedin Academic Press Ltd, p. 340p.
D'Alessandro, A., Bromley, R.G., 1987. Meniscate trace fossils and the *Muensteria–Taenidium* problem. Palaeontology 30, 743–763.
Dalrymple, R.W., Knight, R.J., Zaitlin, B.A., Middleton, G.V., 1990. Dynamics and facies model of a macrotidal sand–bar complex, Cobequid bay—Salmon river estuary (bay of Fundy). Sedimentology 37, 577–612.
Dalrymple, R.W., Zaitlin, B.A., Boyd, R., 1992. Estuarine facies models: conceptual basis and stratigraphic implications. J. Sediment. Petrol. 62, 147–173.
Dalrymple, R.W., Choi, K., 2007. Morphologic and facies trends through the fluvial–marine transition in tide–dominated depositional systems: a schematic framework for environmental and sequence–stratigraphic interpretation. Earth Sci. Rev. 81, 135–174.
Dalrymple, R.W., Kurcinka, C., Jablonski, B., Ichaso, A., Mackay, D., 2015. Deciphering the relative importance of fluvial and tidal processes in the fluvial–marine transition. In: Ashworth, P.J., Best, J.L., Parsons, D.R. (Eds.), *Fluvial–Tidal Sedimentology*. Developments in Sedimentology, vol. 68. Elsevier, pp. 3–45.
Dashtgard, S.E., Gingras, M.K., MacEachern, J.A., 2009. Tidally modulated shorefaces. J. Sediment. Res. 79, 793–807.
Dashtgard, S.E., MacEachern, J.A., Frey, S.E., Gingras, M.K., 2011. Tidal effects on the shoreface: towards a conceptual framework. Sediment. Geol. 279, 42–61.
Dashtgard, S.E., La Croix, A.D., 2015. Sedimentological trends across the tidal–fluvial transition, Fraser River, Canada: a review and some broader implications. In: Ashworth, P.J., Best, J.L., Parsons, D.R. (Eds.), *Fluvial–Tidal Sedimentology*. Developments in Sedimentology, pp. 111–126.
de Gibert, J.M., Martinell, J., Domènech, R., 1995. The rosetted feeding trace fossil *Dactyloidites ottoi* (Geinitz) from the Miocene of Catalonia. Geobios 28 (6), 769–776.
Desjardins, P.R., Buatois, L.A., Mángano, M.G., 2012. Tidal flats and subtidal sand bodies. In: Knaust, D., Bromley, R.G. (Eds.), Trace Fossils as Indicators of Sedimentary Environments, vol. 64. Developments in Sedimentology, pp. 529–561.
Díez–Canseco, D., Buatois, L.A., Mángano, M.G., Rodriguez, W., Solorzano, E., 2015. The ichnology of the fluvial–tidal transition: interplay of ecologic and evolutionary controls. In: Ashworth, P.J., Best, J.L., Parsons, D.R. (Eds.), *Fluvial–Tidal Sedimentology*. Developments in Sedimentology. Elsevier, pp. 283–321.
Dorador, J., Rodríguez-Tovar, F.J., Miguez-Salas, O., 2021. The complex case of *Macaronichnus* trace fossil affecting rock porosity. Sci. Rep. 11, 1975.
Dueñas, H., 1980. Palynology of oligocene-miocene strata of borehole Q-E-22, Planeta Rica, northern Colombia. Rev. Paleobot. Palynol. 30, 313–328.
Dueñas, H., Duque-Caro, H., 1981. Geología del Cuadrángulo F-8 (Planeta Rica). Bol. Geol. - Ingeominas 24 (1), 1–35 (Bogotá).
Dueñas, H., 1983. Fluctuaciones del nivel del mar durante el depósito de los sedimentos basales de la Formación Ciénaga de Oro. Instituto nacional de investigaciones geológico mineras, INGEOMINAS. Bogotá, D.E. Revista de la academia colombiana de ciencias exactas. Físicas Nat. XV, 58.
Dueñas, H., 1986. Geología y palinología de la Formación Ciénaga de Oro, Región Caribe Colombiana, vol. 18. Publicaciones Geológicas Especiales del Ingeominas, Bogotá, pp. 1–56.
Dueñas, H., Gómez, C., 2011. Bioestratigrafía y paleogeografía de la Formación Cansona (Quebrada Peñitas, región Caribe colombiana). In: Memorias XIV Congreso Latinoamericano de Geología y XIII Congreso Colombiano de Geología, Medellin, p. 361.
Duque-Caro, H., 1968. Observaciones generales a la bioestratigrafía y geología regional en los departamentos de Bolívar y Córdoba. Bol. Geol. 24, 71–87.
Duque-Caro, H., 1972. Ciclos tectónicos y sedimentarios en el Norte de Colombia y sus relaciones con la paleoecología. Bol. Geol. - Ingeominas 19, 1–23.
Duque, H., 1973. The geology of the Montería area. In: Annual Field Conference. Society of Petroleum Geology and Geophysics, Bogotá.
Duque–Caro, H., 1991. Contributions to the Geology of the Pacific and the Caribbean Coastal Areas of Northwestern Colombia and South America. Ph.D. Thesis. Princeton University, Nueva Jersey. Estados Unidos, p. 132.
Ekdale, A.A., Bromley, R.G., Pemberton, S.G., 1984. Ichnology: trace fossils in sedimentology and stratigraphy. SEPM Short. Course 15, 317.
Ekdale, A.A., Harding, S.C., 2015. *Cylindrichnus concentricus* Toots in Howard, 1966 (trace fossil) in its type locality, Upper Cretaceous, Wyoming. Ann. Soc. Geol. Pol. 85, 427–432.
Escalona, A., Mann, P., 2011. Tectonics, basin subsidence mechanisms, and paleogeography of the Caribbean-South American plate boundary zone. Mar. Petrol. Geol. 28, 8–39.
Esperante, R., Rodríguez-Tovar, F.J., Nalin, R., 2021. Rhizoliths in lower Pliocene alluvial fan deposits of the Sorbas basin (Almería, SE Spain). Palaeogeogr. Palaeoclimatol. Palaeoecol. 567, 110281.
Flinch, J.F., 2003. Structural evolution of the Sinú-lower Magdalena area (northern Colombia). In: Bartolini, C., Buffler, R.T., Blickwede, J. (Eds.), The Circum-Gulf of

Mexico and the Caribbean: Hydrocarbon Habitats Basin Formation, and Plate Tectonics, vol. 79. AAPG Memoir, pp. 776–796.
Frey, R.W., Howard, J.D., Pryor, W.A., 1978. *Ophiomorpha*: its morphologic, taxonomic, and environmental significance. Palaeogeogr. Palaeoclimatol. Palaeoecol. 23, 199–229.
Frey, R.W., Howard, J.D., 1981. *Conichnus* and *schaubcylindrichnus*: redefined trace fossils from the upper cretaceous of the western interior. J. Paleontol. 55, 800–804.
Frey, R.W., 1990. Trace fossils and hummocky cross-stratification, Upper Cretaceous of Utah. Palaios 5, 203–218.
Fürsich, F.T., 1974. On *Diplocraterion* Torell 1870 and the significance of morphological features in vertical, spreiten-bearing, U-shaped trace fossils. J. Paleontol. 48, 952–962.
Fürsich, F.T., Bromley, R.G., 1985. Behavioural interpretation of a rosetted spreite trace fossil: *Dactyloidites ottoi* (Geinitz). Lethaia 18, 199–207.
Galloway, W.E., 1975. Process framework for describing the morphologic and stratigraphic evolution of deltaic depositional systems. In: Broussard, M.L. (Ed.), Deltas, Models for Exploration, vol. 13. Houston Geological Society, Memories, pp. 87–98.
Gani, M.R., Bhattacharya, J.P., MacEachern, J.A., 2007. Using Ichnology to Determine the Relative Influence of Waves, Storms, Tides, and Rivers in Deltaic Deposits: Examples from Cretaceous Western Interior Seaway, U.S.A. In: MacEachern, J.A., Bann, K.L., Gingras, M.K., Pemberton, S.G. (Eds.), *Applied Ichnology*. Society for Sedimentary Geology, Short Course Notes, vol. 52, pp. 209–225.
García-García, F., Rodríguez-Tovar, F.J., Poyatos-Moré, M., Yeste, L.M., Viseras, C., 2021. Sedimentological and ichnological signatures of an offshore-transitional hyperpycnal system (Upper Miocene, Betic Cordillera, southern Spain). Palaeogeogr. Palaeoclimatol. Palaeoecol. 561, 110039.
Geotec, 2003. Geología de los cinturones Sinú–San Jacinto. Plan 50, 135, 51, 59, 060, 61, 69, 70, 71, 79, 80. Bogotá. Geotec Ldta–Ingeominas.
Giannetti, A., Baeza–Carratalá, J.F., Soria–Mingorance, J.M., Dulai, A., Tent–Manclús, J. E., Peral–Lozano, J., 2018. New paleobiogeographical and paleoenvironmental insight through the Tortonian brachiopod and ichnofauna assemblages from the Mediterranean–Atlantic seaway (Guadix Basin, SE Spain). Facies 64 (3), 24.
Gingras, M.K., MacEachern, J.A., Pemberton, S.G., 1998. A comparative analysis of the ichnology of wave–and river–dominated allomembers of the Upper Cretaceous Dunvegan Formation. Bull. Can. Petrol. Geol. 46, 51–73.
Gingras, M.K., Pemberton, S.G., Saunders, T., Clifton, H.E., 1999. The ichnology of brackish water Pleistocene deposits at Willapa Bay, Washington: variability in estuarine settings. Palaios 14, 352–374.
Gingras, M.K., MacEachern, J.A., Dashtgard, S.E., 2011. Process ichnology and the elucidation of physico–chemical stress. Sediment. Geol. 237, 115–134.
Gingras, M., MacEachern, J.A., 2012. Tidal Ichnology of Shallow–Water Clastic Settings. In: Davis, R.C., Jr., Dalrymple, R.W. (Eds.), Principles of Tidal Sedimentology, vol. 4, pp. 57–77.
Gingras, M.K., MacEachern, J.A., Dashtgard, S.E., 2012. The potential of trace fossils as tidal indicators in bays and estuaries. Sediment. Geol. 279, 97–106.
Goldring, R., Pollard, J.E., Taylor, A.M., 1991. *Anconichnus horizontalis*: a pervasive ichnofabric–forming trace fossil in post–Paleozoic offshore siliciclastic facies. Palaios 6, 250–263.
Goldring, R., Pollard, J.E., 1995. A re–evaluation of *Ophiomorpha* burrows in the Wealden Group (Lower Cretaceous) of southern England. Cretac. Res. 16, 665–680.
Gómez, J., Montes, N.E., Nivia, Á., Diederix, H., 2015. Mapa Geológico de Colombia 2015. Escala 1:1 000 000 (Bogotá. Ingeominas).
Guzmán, G., Gómez, E., Serrano, B.E., 2004. Geología de los cinturones del Sinú, San Jacinto y borde Occidental del Valle Inferior del Magdalena. Caribe Colombiano. Escala 1:300.000, vol. 24. Bogotá., p. 134
Guzmán, G., 2007. Stratigraphy and Sedimentary Environment and Implications in the Plato Basin and the San Jacinto Belt Northwestern Colombia. Ph.D. Thesis. University of Liége, Belgium., p. 275
Hand, B.M., 1997. Inverse grading resulting from coarse-sediment transport lag. J. Sediment. Res. 67, 124–129.
Hansen, C.D., MacEachern, J.A., 2007. Application of the asymmetric delta model to along–strike facies variations in a mixed wave– and river–influenced delta lobe, Upper Cretaceous Basal Belly River Formation, central Alberta. In: MacEachern, J.A., Pemberton, S.G., Gingras, M.K., Bann, K.L. (Eds.), Applied Ichnology. Society for Sedimentary Geology, Tulsa, USA, pp. 256–272.
Hasiotis, S.T., 2010. Continental trace fossils. SEPM Short Course Notes 51, 1–132.
Heldreich, G., Redfern, J., Legler, B., Gerdes, K., Williams, B.P.J., 2017. Challenges in characterizing subsurface paralic reservoir geometries: a detailed case study of the Mungaroo Formation, North West Shelf, Australia. In: Hampson, G.J., Reynolds, A. D., Kostic, B., Wells, M.R. (Eds.), Sedimentology of Paralic Reservoirs: Recent Advances. Geological Society, London, Special Publications, p. 444.
Howard, J.D., 1966. Characteristic trace fossils in upper cretaceous sandstones of the Book Cliffs and Wasatch Plateau. Bull Utah Geol Mineral Surv 80, 35–53.
Howell, J.A., Skorstad, A., MacDonald, A., Fordham, A., Flint, S., Fjellvoll, B., Manzocchi, T., 2008. Sedimentological parameterization of shallow-marine reservoirs. Petrol. Geosci. 14, 17–34.
Husinec, A., Read, J.F., 2011. Microbial laminite versus rooted and burrowed caps on peritidal cycles: Salinity control on parasequence development, Early Cretaceous isolated carbonate platform, Croatia. GSA Bullet. 123, 1896–1907.
Johnson, S.M., Dashtgard, S.E., 2014. Inclined heterolithic stratification in a mixed tidal–fluvial channel: Differentiating tidal versus fluvial controls on sedimentation. Sediment. Geol. 301, 41–53.
Knaust, D., 2009. Ichnology as a tool in carbonate reservoir characterization: a case study from the Permian—Triassic Khuff Formation in the Middle East. GeoArabia 14, 17–38.
Knaust, D., 2015. *Siphonichnidae* (new ichnofamily) attributed to the burrowing activity of bivalves: ichnotaxonomy, behaviour and palaeoenvironmental implications. Earth Sci. Rev. 150, 497–519.
Knaust, D., 2017. Atlas of Trace Fossils in Well Core: Appearance, Taxonomy and Interpretation. Springer, Cham, Switzerland, p. 206.
Knaust, D., 2018. The ichnogenus *Teichichnus* Seilacher, 1955. Earth Sci. Rev. 177, 386–403.
Lazo, D.G., Palma, R.M., Piethé, R.D., 2008. La traza *Dactyloidites ottoi* Geinitz) en la Formación La Manga, Oxfordiano de Mendoza. Ameghiniana 45 (2).
Lowe, D.R., 1976. Grain flow and grain flow deposits. J. Sediment. Petrol. 46, 188–199.
MacEachern, J.A., Stelck, C.R., Pemberton, S.G., 1999. Marine and marginal marine mudstone deposition: Paleoenvironmental interpretations based on the integration of ichnology, palynology and foraminiferal paleoecology. In: Bergman, K.M., Snedden, J.W. (Eds.), Isolated Shallow Marine Sand Bodies: Sequence Stratigraphic and Sedimentologic Interpretation, vol. 64. SEPM, Special Publication, pp. 205–225.
MacEachern, J.A., Bann, K., Bhattacharya, J.P., Howell Jr., C.D., 2005. Ichnology of deltas: organism responses to the dynamic interplay of rivers, waves, storms and tides. In: Bhattacharya, B.P., Giosan, L. (Eds.), River Deltas: Concepts, Models and Examples, vol. 83. SEPM Special Publication, pp. 45–85.
MacEachern, J.A., Gingras, M.K., 2007. Recognition of brackish–water trace–fossil suites in the Cretaceous Western Interior Seaway of Alberta, Canada. In: Bromley, R.G., Buatois, L.A., Mángano, M.G. (Eds.), Sediment–organism Interactions: a Multifaceted Ichnology, vol. 88. SEPM Special Publication, pp. 149–193.
MacEachern, J.A., Bann, K.L., Pemberton, S.G., Gingras, M.K., 2007a. The ichnofacies paradigm: high–resolution paleoenvironmental interpretation of the rock record. In: MacEachern, J.A., Bann, K.L., Gingras, M.K., Pemberton, S.G. (Eds.), *Applied Ichnology*. Society for Sedimentary Geology, Short Course Notes, vol. 52, pp. 27–64.
MacEachern, J.A., Pemberton, S.G., Gingras, M.K., Bann, K.L., Dafoe, L.T., 2007b. Use of trace fossils in genetic stratigraphy. In: Miller III., W. (Ed.), Trace Fossils: Concepts, Problems, Prospects. Elsevier, pp. 110–134.
MacEachern, J.A., Bann, K.L., 2008. The role of ichnology in refining shallow marine facies models. In: Hampson, G.J., Steel, R.J., Burgess, P.M., Dalrymple, R.W. (Eds.), Recent Advances in Models of Siliciclastic Shallow-Marine Stratigraphy, vol. 90. SEPM Special Publication No, pp. 73–116.
MacEachern, J.A., Bann, K.L., 2020. The *Phycosiphon* Ichnofacies and the *Rosselia* Ichnofacies: Two new Seilacherian Ichnofacies for marine deltaic environments. J. Sediment. Res. 90, 855–886.
Manco–Garcés, A., Marín–Cerón, M.I., Sánchez–Plazas, C.J., Escobar–Arenas, L.C., Beltrán–Triviño, A., von Quadt, A., 2020. Provenance of the Ciénaga de Oro Formation: unveiling the tectonic evolution of the Colombian Caribbean margin during the Oligocene - Early Miocene. Bol. Geol. 42 (3), 205–226.
Marín, J.P., Bermúdez, H.D., Aguilera, R., Jaramillo, J.M., Rodríguez, J.V., Ruiz, E.C., Cerón, M.R., 2010. Evaluación geológica y prospectividad sector Sinú – Urabá. Bol. Geol. 32 (1), 145–153.
Maselli, V., Normandeau, A., Nones, M., Tesi, T., Langone, L., Trincardi, F., Bohacs, K.M., 2020. Tidal modulation of river–flood deposits: How low can you go? Geology 48, 663–667.
Melchor, R.N., Genise, J.F., Buatois, L.A., Umazano, A.M., 2012. Fluvial environments. In: Knaust, D., Bromley, R.G. (Eds.), Trace Fossils as Indicators of Sedimentary Environments. Developments in Sedimentology, vol. 64, pp. 329–378.
Miall, A.D., 1988. Reservoir heterogeneities in fluvial sandstones: lessons from outcrop studies. AAPG (Am. Assoc. Pet. Geol.) Bull. 72, 682–697.
Miguez–Salas, O., Rodríguez–Tovar, F.J., 2019. Stable deep–sea macrobenthic trace maker associations in disturbed environments from the Eocene Lefkara Formation, Cyprus. Geobios 52, 37–45.
Miguez–Salas, O., Rodríguez–Tovar, F.J., De Weger, W., 2020. *Macaronichnus* and contourite depositional settings: Bottom currents and nutrients as coupling factors. Palaeogeogr. Palaeoclimatol. Palaeoecol. 545, 109639.
Molinares, C.E., Martinez, J.I., Fiorini, F., Escobar, J., Jaramillo, C., 2012. Paleoenvironmental reconstruction for the Lower Pliocene Arroyo Piedras section (Tubará – Colombia): Implications for the Magdalena River – paleodelta's Dynamic. J. S. Am. Earth Sci. 39, 170–183.
Monaco, P., Caracuel, J.E., Giannetti, A., Soria, J.M., Yébenes, A., 2009. *Thalassinoides* and *Ophiomorpha* as cross–facies trace fossils of crustaceans from shallow–to–deep–water environments: Mesozoic and Tertiary examples from Italy and Spain. In: Garassino, A., Feldmann, R.M., Teruzzi, G. (Eds.), *3rd Symposium on Mesozoic and Cenozoic Decapod Crustaceans—Museo di Storia Naturale di Milano*, May 23–25, 2007, vol. 35. Memorie della Società Italiana di Scienze Naturali e del Museo Civico di Storia Naturale di Milano, pp. 79–82.
Montes, C., Rodriguez–Corcho, A.F., Bayona, G., Hoyos, N., Zapata, S., Cardona, A., 2019. Continental margin response to multiple arc–continent collisions: The northern Andes–Caribbean margin. Earth Sci. Rev. 198, 102903.
Mora, J.A., Oncken, O., Le Breton, E., Ibánez–Mejia, M., Faccena, C., Veloza, G., Vélez, V., de Freitas, M., Mesa, A., 2017. Linking Late Cretaceous to Eocene tectonostratigraphy of the San Jacinto fold belt of NW Colombia with Caribbean plateau collision and flat subduction. Tectonics 36, 2599–2629.
Mora, J.A., Oncken, O., Le Breton, E., Mora, A., Veloza, G., Vélez, V., de Freitas, M., 2018. Controls on forearc basin formation and evolution: Insights from Oligocene to Recent tectonostratigraphy of the Lower Magdalena Valley basin of northwest Colombia. Mar. Petrol. Geol. 97, 288–310.
Mora–Páez, H., Kellogg, J.N., Freymueller, J., Mencin, D., Fernandes, R.M.S., Diederix, H., LaFemina, P., Cardona–Piedrahita, L., Lizarazo, S., Peláez–Gaviria, J.-R., Díaz–Mila, F., Bohórquez–Orozco, O., Giraldo–Londoño, L., Corchuelo–Cuervo, Y., 2019. Crustal deformation in the northern Andes – A new GPS velocity field. J. S. Am. Earth Sci. 89, 76–91.

Moslow, T.F., Pemberton, S.G., 1988. An integrated approach to the sedimentological analysis of some Lower Cretaceous shoreface and delta front sandstone sequences. In: James, D.P., Leckie, D.A. (Eds.), Sequences, Stratigraphy, Sedimentology: Surface and Subsurface, vol. 15. Canadian Society of Petroleum Geologists, Memoir, pp. 373–386.

Moyano Paz, D., Richiano, S., Varela, A.N., Gómez Decál, A.R., Poiré, D.G., 2020. Ichnological signatures from wave– and fluvial–dominated deltas: The La Anita Formation, Upper Cretaceous, Austral–Magallanes Basin, Patagonia. Mar. Petrol. Geol. 114, 104168.

Mulder, T., Syvitski, J.P.M., 1995. Turbidity currents generated at river mouths during exceptional discharges to the world oceans. J. Geol. 103, 285–298.

Mulder, T., Syvitski, J.P.M., Migeon, S., Faugères, J.C., Savoye, B., 2003. Marine hyperpycnal flows: initiation, behavior and related deposits: A review. Mar. Petrol. Geol. 20, 861–882.

Nara, M., Seike, K., 2004. *Macaronichnus segregatis–like* traces found in the modern foreshore sediments of the Kujukurihama Coast, Japan. J. Geol. Soc. Jpn. 110, 545–551.

Naruse, H., Nifuku, K., 2008. Three–dimensional morphology of the ichnofossil *Phycosiphon incertum* and its implication for paleoslope inclination. Palaios 23, 270–279.

Nemec, W., Postma, G., 1993. Quaternary alluvial fans in southwestern Crete: sedimentation processes and geomorphic evolution. In: Marzo, M., Puigdefabregas, C. (Eds.), *Alluvial Sedimentation*. International Association of Sedimentologists, vol. 17. Special Publications, pp. 235–276.

Netto, R.G., Rossetti, D. de F., 2003. Ichnology and salinity fluctuations: a case study from the early Miocene (Lower Barreiras Formation) of São Luís Basin, Maranhão, Brazil. Rev. Bras. Palaontol. 6, 5–18.

Nichols, G., 2009. Sedimentology and Stratigraphy. Blackwell Publishing, A John Wiley and Sons, Ltd., Publication, p. 432.

Osorno, J., Rangel, A., 2015. Geochemical Assessment and Petroleum Systems in the Sinú-San Jacinto Basin, Northwestern Colombia. Mar. Petrol. Geol. 65, 217–231.

Orton, G.J., Reading, H.G., 1993. Variability of deltaic processes in terms of sediment supply, with particular emphasis on grain size. Sedimentology 40, 475–512.

Osorio-Granada, E., Pardo-Trujillo, A., Restrepo-Moreno, S.A., Gallego, F., Muñoz, J., Plata, A., Trejos-Tamayo, R., Vallejo, F., Barbosa-Espitia, A., Cardona-Sánchez, F.J., Foster, D.A., Kamenov, G., 2020. Provenance of Eocene-Oligocene sediments in the San Jacinto Fold Belt: Paleogeographic and geodynamic implications for the northern Andes and the southern Caribbean. Geosphere 16 (1), 210–228.

Pardo–Trujillo, A., Cardona, A., Giraldo, S.A., León, S., Vallejo, D.F., Trejos–Tamayo, R., Plata, A., Ceballos, J., Echeverri, S., Barbosa–Espitia, A., Slattery, J., Salazar–Ríos, A., Botello, G.E., Celis, S.A., Osorio–Granada, E., Giraldo–Villegas, C. A., 2020. Sedimentary record of the Cretaceous–Paleocene arc–continent collision in the northwestern Colombian Andes: insights from stratigraphic and provenance constraints. Sediment. Geol. 401, 105627.

Pemberton, S.G., Frey, R.W., 1984. Ichnology of storm-influenced shallow marine sequence: Cardium Formation (Upper Cretaceous) at Seebe, Alberta. In: Stott, D.F., Glass, D.J. (Eds.), The Mesozoic of Middle North America, vol. 9. *Canadian Society of Petroleum Geologists*, Memoir, pp. 281–304.

Pemberton, S.G., MacEachern, J.A., Ranger, M.J., 1992. Ichnology and event stratigraphy: the use of trace fossils in recognizing tempestites. In: Pemberton, S.G. (Ed.), Applications of Ichnology to Petroleum Exploration. A Core Workshop, vol. 17. SEPM Core Workshop, pp. 85–117.

Pemberton, S.G., Wightman, D.M., 1992. Ichnological characteristics of brackish water deposits. In: Pemberton, S.G. (Ed.), *Applications Of Ichnology To Petroleum Exploration*. A Core Workshop, vol. 17. SEPM, pp. 141–167.

Pemberton, S.G., Spila, M., Pulham, A.J., Saunders, T., MacEachern, J.A., Robbins, D., Sinclair, I.K., 2001. *Ichnology and sedimentology of shallow to marginal marine systems*. Ben Nevis and Avalon Reservoirs, Jeanne dArc Basin. Geological Association of Canada. Short Course Notes 15, 343.

Picard, M.D., High, L.R., 1973. Sedimentary Structures of Ephemeral Streams. Elsevier, Amsterdam, p. 223p.

Pindell, J., Kennan, L., Maresch, W.V., Draper, G., 2005. Plate–kinematics and crustal dynamics of circum–Caribbean arc–continent interactions: Tectonic controls on basin development in Proto–Caribbean margins. Geol. Soc. Am. Spec. Pap. 394 (1), 7–52.

Pollard, J.E., Goldring, R., Buck, S.G., 1993. Ichnofabrics containing *Ophiomorpha*: significance in shallow–water facies interpretation. J. Geol. Soc. 150, 149–164.

Pratt, B.R., 1998. Syneresis cracks: subaqueous shrinkage in argillaceous sediments caused by earthquake-induced dewatering. Sediment. Geol. 117, 1–10.

Potter, P.E., Maynard, J.B., Depetris, P.J., 2005. Mud and Mudstones: Introduction and Overview. Springer Berlin/Heidelberg, p. 297p.

Project Contrato RC 494, 2017. Informe de integración del proyecto “Certificación de estratigrafía física y de edad de los núcleos de perforación recuperados por la Agencia Nacional de Hidrocarburos en las cuencas de Sinú-San Jacinto y cordillera”. Universidad de Caldas - Ministerio de Ciencia, Tecnología e Innovación Minciencias - Agencia Nacional de Hidrocarburos ANH. Informe confidencial.

Quiroz, L.I., Buatois, L.A., Mángano, M.G., Jaramillo, C.A., Santiago, N., 2010. Is the trace fossil *Macaronichnus segregatis* an indicator of temperate to cold waters? Exploring the paradox of its occurrence in tropical coasts. Geology 38, 651–654.

Quiroz, L.I., Buatois, L.A., Seike, K., Mángano, M.G., Jaramillo, C., Sellers, A., 2019. The search for an elusive worm in the tropics, the past as a key to the present, and reverse uniformitarianism. Sci. Rep. 9, 18402.

Reading, H., 1996. Sedimentary Environments: Processes, Facies and Stratigraphy, third ed. Blackwell Scientific Ltd, Oxford, p. 689p.

Retallack, G.J., 2001. Soils of the Past: an Introduction to Paleopedology. Blackwell Science, Oxford, p. 549.

Rodríguez–Tovar, F.J., Puga–Bernabéu, A., Buatois, L.A., 2008. Large burrow systems in marine Miocene deposits of the Betic Cordillera (Southeast Spain). Palaeogeogr. Palaeoclimatol. Palaeoecol. 268, 19–25.

Rodríguez–Tovar, F.J., Aguirre, J., 2014. Is *Macaronichnus* an exclusively small, horizontal and unbranched structure? *Macaronichnus segregatis degiberti isubsp*. Nov. Spanish J. Palaeontol. 29, 131–142.

Rodríguez–Tovar, F.J., Nagy, J., Reolid, M., 2014. Palaeoenvironment of Eocene prodelta in Spitsbergen recorded by the trace fossil *Phycosiphon incertum*. Polar Res. 33, 23786.

Rodríguez–Tovar, F.J., Alcalá, L., Cobos, A., 2016. *Taenidium* at the lower Barremian El Hoyo dinosaur tracksite (Teruel Spain): assessing palaeoenvironmental conditions for the invertebrate community. Cretac. Res. 65, 48–58.

Rodríguez–Tovar, F.J., Miguez–Salas, O., Duarte, L.V., 2017. Toarcian Oceanic Anoxic Event induced unusual behaviour and palaeobiological changes in *Thalassinoides* tracemakers. Palaeogeogr. Palaeoclimatol. Palaeoecol. 485, 46–56.

Rosello, E., Cossey, S., 2012. What is the evidence for subduction in the Caribbean Margin of Colombia?. In: Extended abstract in Memoirs of the XII Simposio Bolivariano de Cuencas Subandinas: Cartagena, Colombia. Asociación Colombiana de Geólogos y Geofísicos del Petróleo, pp. 1–7.

Savrda, C.E., Ozalas, K., Demko, T.H., Hichison, R.A., Scheiwe, T.D., 1993. Log–grounds and the ichnofossil *Teredolites* in transgressive deposits of the Clayton Formation (Lower Paleocene), Western Alabama. Palaios 8, 311–324.

Savrda, C.E., Blanton–Hooks, A.D., Collier, J.W., Drake, R.A., Graves, R.L., Hall, A.G., Nelson, A.J., Slone, J.C., Williams, D.D., Wood, H.A., 2000. *Taenidium* and associated ichnofossils in fluvial deposits, Cretaceous Tuscaloosa Formation, eastern Alabama, southeastern USA. Ichnos 7, 777–806.

Savrda, C.E., 2002. Equilibrium responses reflected in a large *Conichnus* (Upper Cretaceous Eutaw Formation, Alabama, USA). Ichnos 9, 33–40.

Shanmugam, G., 1997. The Bouma Sequence and the turbidity mindset. Earth Sci. Rev. 42, 201–229.

Shchepetkina, A., Gingras, M.K., Mángano, M.G., Buatois, L.A., 2019. Fluvio–tidal transition zone: Terminology, sedimentological and ichnological characteristics, and significance. Earth Sci. Rev. 192, 214–235.

Schultz, S.K., MacEachern, J.A., Catuneanu, O., Dashtgard, S., 2020. Coeval deposition of transgressive and normal regressive stratal packages in a structurally controlled area of the Viking Formation, central Alberta, Canada. Sedimentology. https://doi.org/10.1111/sed.12730.

Seike, K., 2007. Palaeoenvironmental and palaeogeographical implications of modern *Macaronichnus segregatis*–like traces in foreshore sediments on the Pacific coast of central Japan. Palaeogeogr. Palaeoclimatol. Palaeoecol. 252, 497–502.

Shields, D.J., Strobl, R., 2010. The Wabiskaw D Member, Clearwater Formation: A World Class Oil Sands Reservoir Hosted in an Incised Valley Complex. In: GeoCanada 2010 – Working with the Earth. AAPG, p. 5.

Silva–Arias, A., Páez–Acuña, L.A., Rincón–Martínez, D., Tamara–Guevara, J.A., Gomez–Gutierrez, P.D., López–Ramos, E., Restrepo–Acevedo, S.M., Mantilla–Figueroa, L.-C., Valencia, V., 2016. Basement characteristics in the Lower Magdalena Valley and the Sinú and San Jacinto Fold Belts: evidence of a Late Cretaceous magmatic arc at the South of the Colombian Caribbean. Cienc. Tecnol. Fut. 6, 5–36.

Silva–Tamayo, J.C., Lara, M.E., Yobo, L.N., Erdal, Y.D., Sanchez, J., Zapata–Ramírez, P. A., 2017. Tectonic and environmental factors controlling on the evolution of Oligo – Miocene shallow marine carbonate factories along a tropical SE Circum–Caribbean. J. S. Am. Earth Sci. 78, 213–237.

Slatt, R.M., 2006. Geologic controls on reservoir quality. In: Slatt, R.M. (Ed.), Stratigraphic Reservoir Characterization for Petroleum Geologists, Geophysicists, and Engineers, vol. 61. Elsevier, Amsterdam, pp. 159–202.

Solórzano, E.J., Buatois, L.A., Rodríguez, W.J., Mángano, M.G., 2017. From freshwater to fullymarine: Exploring animal-substrate interactions along a salinity gradient (Miocene Oficina Formation of Venezuela). Palaeogeogr. Palaeoclimatol. Palaeoecol. 482, 30–47.

Taboada, A., Rivera, L.A., Fuenzalida, A., Cisternas, A., Philip, H., Olaya, J., Rivera, C., 2000. Geodynamics of the northern Andes: Subductions and intracontinental deformation (Colombia). Tectonics 19 (5), 787–813.

Tanner, P.W.G., 2003. Syneresis. In: Middleton, G.V. (Ed.), Encyclopedia of Sediments and Sedimentary Rocks. Kluwer Academic, Dordrecht, pp. 718–720.

Taylor, A.M., Goldring, R., 1993. Description and analysis of bioturbation and ichnofabric. J. Geol. Soc. Lond. 150, 141–148.

Taylor, A., Goldring, R., Gowland, S., 2003. Analysis and application of ichnofabrics. Earth Sci. Rev. 60, 227–259.

Todd, S.P., 1989. Stream-driven, high-density gravelly traction carpets: possible deposits in the Trabeg Conglomerate Formation, SW Ireland and some theoretical considerations of their origin. Sedimentology 36, 513–530.

Tonkin, N.S., 2012. Deltas. In: Knaust, D., Bromley, R.G. (Eds.), Trace Fossils as Indicators of Sedimentary Environments. Developments in Sedimentology, vol. 64, pp. 507–528, 17.

Uchman, A., Pervesler, P., 2007. Palaeobiological and palaeonvironmental significance of the Pliocene trace fossil *Dactyloidites peniculus*. Acta Palaeontol. Pol. 52 (4), 799–808.

Uchman, A., 2009. The *Ophiomorpha rudis* ichnosubfacies of the Nereites ichnofacies: characteristics and constraints. Palaeogeogr. Palaeoclimatol. Palaeoecol. 276, 107–119.

Uchman, A., Johnson, M.E., Rebelo, A.C., Melo, C., Cordeiro, R., Ramalho, R.C., Ávila, S. P., 2016. Vertically–oriented trace fossil *Macaronichnus segregatis* from Neogene of Santa Maria Island (Azores; NE Atlantic) records vertical fluctuations of the coastal groundwater mixing zone on a small oceanic island. Geobios 49, 229–241.

Wetzel, A., Bromley, R.G., 1994. *Phycosiphon incertum* revisited: *Anconichnus* horizontalis is its junior subjective synonym. J. Paleontol. 68, 1396–1402.
Wetzel, A., 2008. Recent bioturbation in the deep South China Sea: a uniformitarian ichnologic approach. Palaios 23, 601–615.
Wetzel, A., 2010. Deep-sea ichnology: observations in modern sediments to interpret fossil counterparts. Acta Geol. Pol. 60, 125–138.
Whateley, M.K.G., Pickering, K.T., 1989. Deltas: Sites and Traps for Fossil Fuels, vol. 41. Geological Society London, Special Publication, p. 360.
Whybrow, P.J., McClure, H.A., 1980. Fossil mangrove roots and palaeoenvironments of the Miocene of the eastern Arabian Peninsula. Palaeogeogr. Palaeoclimatol. Palaeoecol. 32, 213–225.
Zavala, C., Arcuri, M., Di Meglio, M., Gamero Diaz, H., Contreras, C., 2011. A genetic facies tract for the analysis of sustained hyperpycnal flow deposits. In: Slatt, R.M., Zavala, C. (Eds.), Sediment Transfer from Shelf to Deep Water Revisiting the Delivery System. AAPG Studies in Geology, vol. 61, pp. 31–51.
Zavala, C., Pan, S.X., 2018. Hyperpycnal flows and hyperpycnites: Origin and distinctive characteristics. Lithol. Reserv. 3 (1), 1–27.